

Article



https://doi.org/10.11646/zootaxa.4718.2.1 http://zoobank.org/urn:lsid:zoobank.org:pub:DE6C3BAE-640A-447C-AE23-4145654DD68C

Two new species of *Cyrtodactylus* Gray, 1827 (Squamata: Gekkonidae) from a karstic archipelago in the Salween Basin of southern Myanmar (Burma)

L. LEE GRISMER^{1*}, PERRY L. WOOD, JR.², EVAN S.H. QUAH^{1,3}, MARTA S. GRISMER¹, MYINT KYAW THURA⁴, JAMIE R. OAKS² & AUNG LIN⁵

¹Herpetology Laboratory, Department of Biology, La Sierra University, 4500 Riverwalk Parkway, Riverside, California 92515, USA. lgrismer@lasierra.edu

²Department of Biological Sciences & Museum of Natural History, Auburn University, Auburn, Alabama 36849, USA Email: jro0014@ auburn.edu; perryleewoodjr@gmail.com

³Institute of Tropical Biodiversity and Sustainable Development, Universiti Malaysia Terengganu, 21030 Kuala Nerus, Terengganu, Malaysia. Email: evanquah@umt.edu.my

⁴Myanmar Environment Sustainable Conservation, Yangon, Myanmar. Email: mgmyint.banca@gmail.com

⁵Fauna and Flora International, No(35), 3rd Floor, Shan Gone Condo, Myay Ni Gone Market Street, Sanchaung Township, Yangon, Myanmar. Email: aung.lin@fauna-flora.org

Abstract

An integrative taxonomic analysis of the 10 species of the *Cyrtodactylus sinyineensis* group based on squamation, color pattern, and the mitochondrial gene NADH dehydrogenase subunit 2 (ND2) and its flanking tRNA regions, recovered the newly discovered populations from Datt Kyaik and Taung Wine Hills in Kayin State as the new species *Cyrtodactylus dattkyaikensis* **sp. nov.** and *C. taungwineensis* **sp. nov.** The Maximum Likelihood and Bayesian phylogenetic estimates supported *C. dattkyaikensis* **sp. nov.** as the sister species of *C. bayinnyiensis* and *C. taungwineensis* **sp. nov.** as the sister species of *C. sinyineensis*. Each new species is differentially diagnosable from all other *C. sinyineensis* group species based on their morphological placement in multivariate space and several statistically significant mean differences is meristic squamation and color pattern data. The *C. sinyineensis* group ranges across an archipelago of karstic habitat-islands in the Salween Basin of southern Myanmar. The discovery of these new species continues to underscore the unprecedented high degree of diversity and site-specific endemism in this relatively small region and the urgent need for the conservation of its karstic terranes.

Key words: Integrative taxonomy, Systematics, Southeast Asia, habitat islands, limestone

Introduction

Field work and phylogenetic studies on the herpetofauna of the Salween Basin in southern Myanmar (Fig. 1) have shown that this relatively small and physiographically circumscribed landscape has been a region of multiple, independent, adaptive radiations of different clades of karst-associated Bent-toed Geckos (genus *Cyrtodactylus* Gray) (Grismer *et al.* 2018a,b). Grismer *et al.* (2018a) noted that the unique geomorphology of the basin's interior—bearing dozens of scattered limestone hills and towers—have been foci for speciation and have generated an unprecedented degree of diversity and site-specific endemism across this archipelago of karstic habitat-islands. In their initial descriptions of 12 new species and the designation of three new species groups, Grismer *et al.* (2018a,b) noted that multiple, unrelated species from different species groups occupied some of the same karstic islands, indicating they were colonized independently and at different periods in time (see Grismer *et al.* 2018c). More importantly, however, they noted there were at least 44 isolated habitat-islands that have not been surveyed and thus the potential herpetological diversity of this region is far from being realized.

As part of our team's efforts to survey karstic landscapes throughout Myanmar, we visited four habitat islands in the northern Salween Basin in Kayin and Mon states during November 2018 and discovered two new populations of *Cyrtodactyus* from two small, unsurveyed karstic hills—Datt Kyaik and Taung Wine (Fig. 2). Morphological comparisons placed these populations within the *C. sinyineensis* group (*sec.* Grismer *et al.* 2018a; see below), however,

neither population could be ascribed to any known species within that group. Molecular phylogenetic analyses using the mitochondrial gene NADH dehydrogenase subunit 2 (ND2) and its flanking tRNA regions also recovered these populations as new monophyletic lineages within the *C. sinyineensis* group. Additionally, multivariate and univariate statistical analyses of squamation and color pattern consistently differentiated these lineages from all previously described species recovered in the phylogenetic analyses. As such, we put forward testable hypotheses proposing that each new population represents a new species that we describe herein.

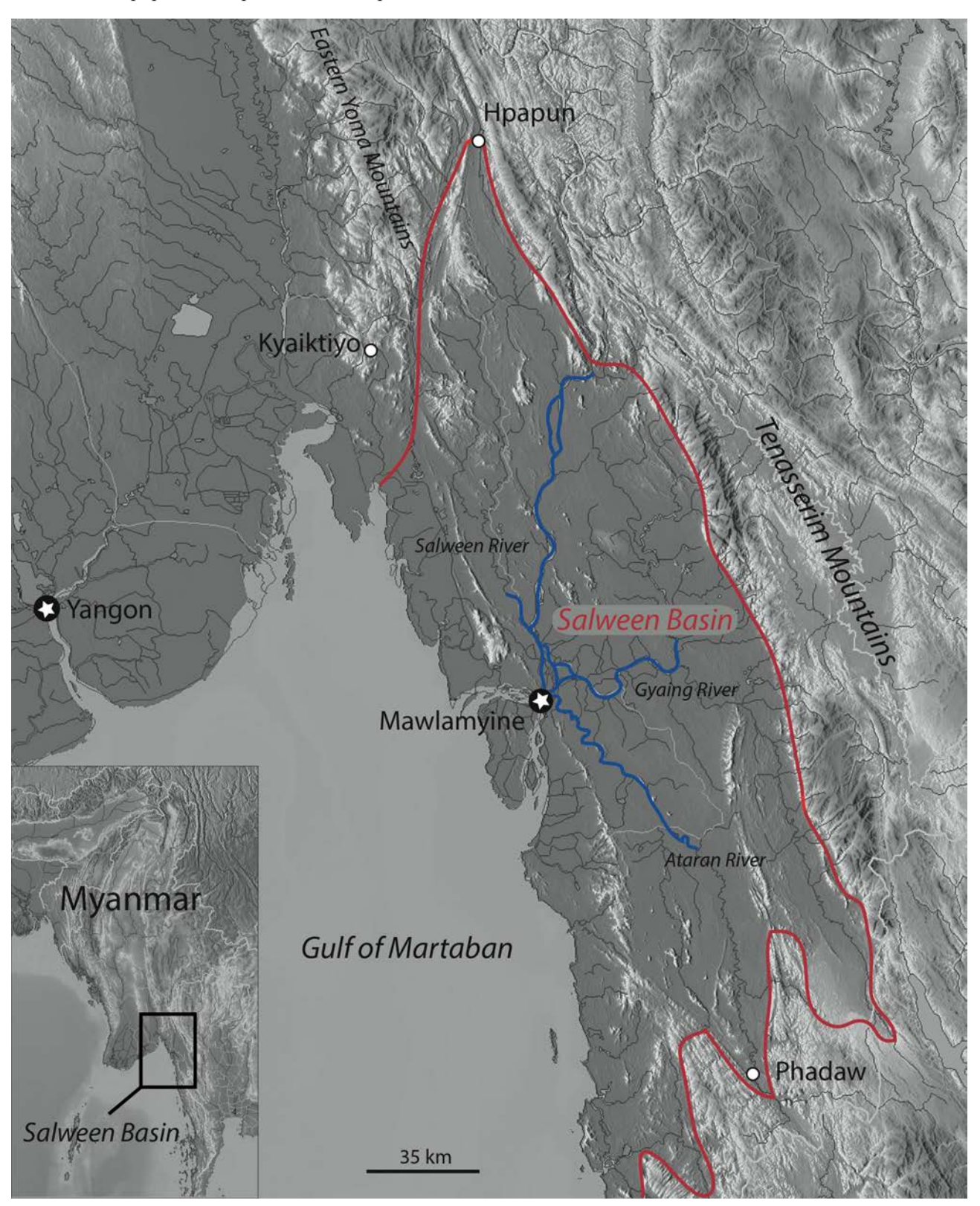


FIGURE 1. Location and general limits (red) of the Salween Basin in southern Myanmar.

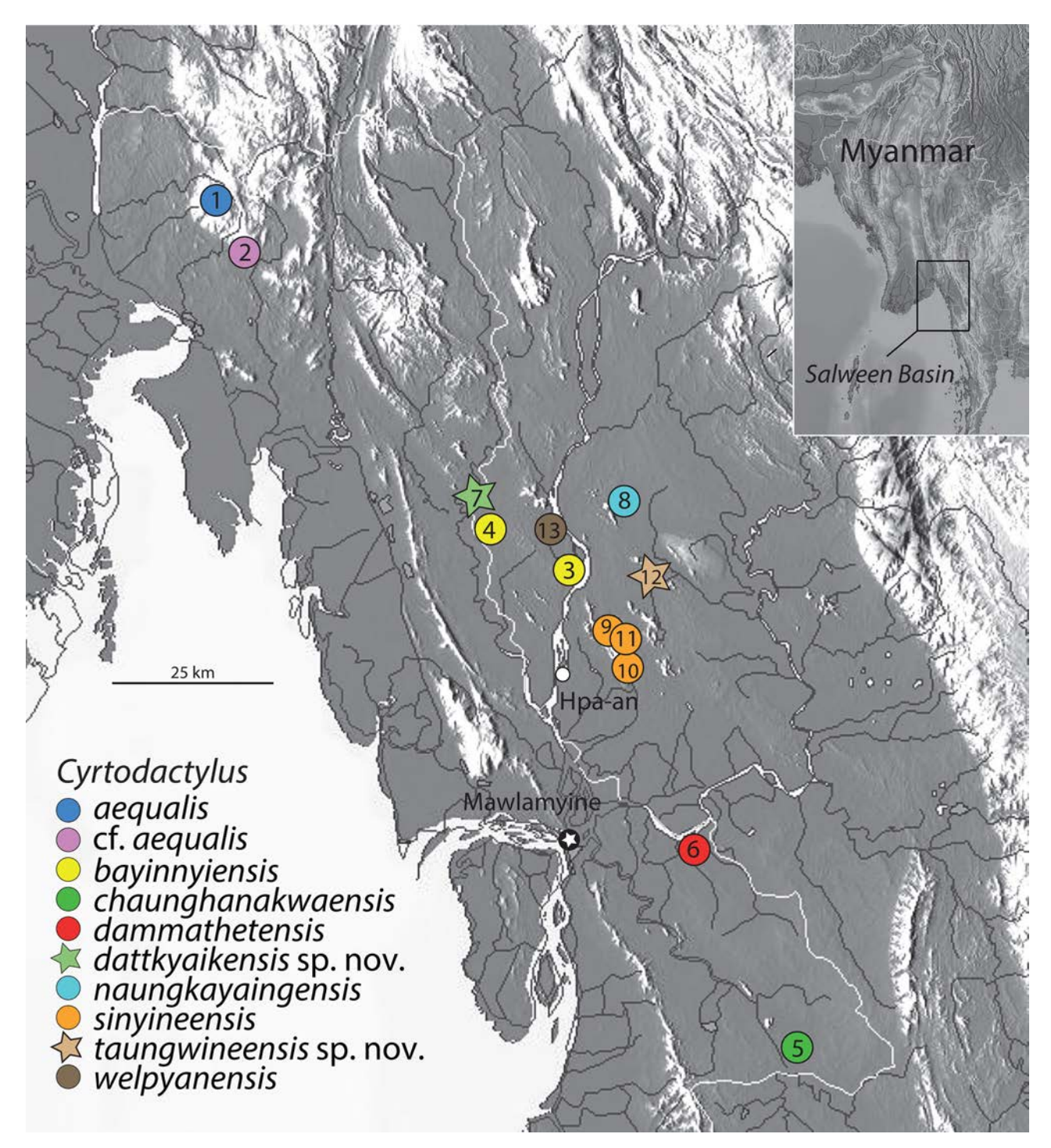


FIGURE 2. Distribution of the species of the *Cyrtodactylus sinyineensis* group. 1. Kyaiktiyo Hill, Mon State, Myanmar (17.28819°N, 97.05974°E). 2. Kay Lar Tha Hill, Mon State, Myanmar (17.22223°N, 97.09014°E). 3. Hpa-pu Hill 3.1 km north of Hpa-an, Kayin State, Myanmar (16.91072°N, 97.62716°E). 4. Bayin Nyi Cave 16.8 km northwest of Hpa-an, Kayin State, Myanmar (16.97048°N, 97.49378°E). 5. Chaunghanakwa Hill approximately 50 km southeast of Mawlamyine, Mon State, Myanmar (16.18456°N, 97.98814°E). 6. Dammathet Cave 19.8 km east of Mawlamyine, Mon State, Myanmar (16.30380°N, 97.48629°E). 7. Datt Kyaik Cave, Kayin State, Myanmar (17.02854°N, 97.47071°E). 8. Naung Ka Yaing Hill, 17 km northeast of Hpa-an, Kayin State, Myanmar (17.01558°N, 97.70641°E). 9. Sin Yine Cave 18.5 km southeast of Hpa-an, Kayin State, Myanmar (16.44605°N, 97.29493°E). 10. Zwegabin Mountain, Kayin State, Myanmar (16.82407°N, 97.66810°E). 11. Kok Ka Thaung, Kayin State, Myanmar (16.82854°N, 97.70561°E). 12. Taung Wine Mountain, Kayin State, Myanmar (16.90932°N, 97.74842°E). 13. Wel Pyan Cave 35 km north of Hpa-an, Kayin State, Myanmar (17.1288°N, 97.37066°E).

Materials and methods

Species delimitation. The general lineage concept (GLC: de Queiroz 2007) adopted herein proposes that a species constitutes a population of organisms evolving independently from other such populations owing to a lack of gene flow. By "independently," it is meant that new mutations arising in one species cannot spread readily into another species (Barraclough *et al.* 2003 and de Queiroz 2007). Integrative studies on the nature and origins of species are using an increasingly wider range of empirical data to delimit species boundaries (Coyne & Orr 1998; Fontaneto *et al.* 2007; Knowles & Carstens 2007; Leaché *et al.* 2009), rather than relying solely on morphology and traditional taxonomic methods. Under the GLC implemented herein, molecular phylogenies were used to recover monophyletic mitochondrial lineages of individuals (populations) in order to develop initial species-level hypotheses—the grouping stage of Hillis (2019). Discrete color pattern data and univariate and multivariate analyses of morphological data were then used to search for characters and morphospatial patterns bearing statistically significant differences that were consistent with the previous designations of the species-level hypotheses—the construction of boundaries representing the hypothesis-testing step of Hillis (2019)—thus providing independent diagnoses to complement the molecular analyses.

Molecular data. The primary aim of this study was to investigate the taxonomy and phylogenetic relationships of the newly discovered populations of *Cyrtodactylus* of the *C. sinyineensis* group from the northern Salween Basin based on 1479 bp of ND2 and its flanking tRNAs (WANCY region). The data set of Grismer *et al.* (2019a), which included exemplars of all the major *Cyrtodactylus* clades in Wood *et al.* (2012) and Agarwal *et al.* (2014), was augmented with the following newly sampled material (Table 1): 14 specimens from Taung Wine Hill, Kayin State; three specimens from Datt Kyaik Hill, Kayin State; 15 *C. aequalis* from Mon State; four *C. cf. aequalis* (see below for cf. designation), from Mon State; and six *C. sinyineensis* from Zwegabin Mounatin, Kayin State totaling 319 ingroup samples (tips). *Hemidactylus angulatus* Hallowell, *H. frenatus* Duméril & Bibron, *H. garnotii* Duméril & Bibron, *H. mabouia* (Moreau de Jonnès), and *H. turcicus* (Linnaeus) served as outgroups following Grismer *et al.* (2019a,b). The new *C. sinyineensis* group sequences were deposited in GenBank (Table 1).

TABLE 1. GenBank accession numbers for the newly recorded specimens and all species in the *Cyrtodactylus sinyineensis* group used for the molecular phylogenetic analyses. Accession numbers for outgroups are in Agarwal *et al.* (2014) and for the other specimens of *Cyrtodactylus* of the Indochina clade see Grismer *et al.* (2018a,b). Numbers in parentheses refer to locations in Figure 1.

			GenBank
Taxon	Catalog no.	Locality	no.
Cyrtodactylus aequalis (1)	LSUHC 12895	Kyaiktiyo Hill, Mon State, Myanmar (17.28819°N, 97.05974°E)	MN534915
Cyrtodactylus aequalis (1)	LSUHC 14052	Kyaiktiyo Hill, Mon State, Myanmar (17.28819°N, 97.05974°E)	MN534916
Cyrtodactylus aequalis (1)	LSUHC 14057	Kyaiktiyo Hill, Mon State, Myanmar (17.28819°N, 97.05974°E)	MN534917
Cyrtodactylus aequalis (1)	LSUHC 14055	Kyaiktiyo Hill, Mon State, Myanmar (17.28819°N, 97.05974°E)	MN534918
Cyrtodactylus aequalis (1)	LSUHC 14064	Kyaiktiyo Hill, Mon State, Myanmar (17.28819°N, 97.05974°E)	MH198649
Cyrtodactylus aequalis (1)	LSUHC 14061	Kyaiktiyo Hill, Mon State, Myanmar (17.28819°N, 97.05974°E)	MH198651
Cyrtodactylus aequalis (1)	LSUHC 14062	Kyaiktiyo Hill, Mon State, Myanmar (17.28819°N, 97.05974°E)	MH198650
Cyrtodactylus aequalis (1)	LSUHC 14063	Kyaiktiyo Hill, Mon State, Myanmar (17.28819°N, 97.05974°E)	MH198649
Cyrtodactylus aequalis (1)	LSUHC 14053	Kyaiktiyo Hill, Mon State, Myanmar (17.28819°N, 97.05974°E)	MN534913
Cyrtodactylus aequalis (1)	LSUHC 14054	Kyaiktiyo Hill, Mon State, Myanmar (17.28819°N, 97.05974°E)	MN534909

TABLE 1. (Continued)

Taxon	Catalog no.	Locality	GenBank no.		
Cyrtodactylus aequalis (1)	LSUHC 14056	Kyaiktiyo Hill, Mon State, Myanmar (17.28819°N, 97.05974°E)	MN534910		
Cyrtodactylus aequalis (1)	LSUHC 14058	Kyaiktiyo Hill, Mon State, Myanmar (17.28819°N, 97.05974°E)	MN534911		
Cyrtodactylus aequalis (1)	LSUHC 14059	Kyaiktiyo Hill, Mon State, Myanmar (17.28819°N, 97.05974°E)	MN534912		
Cyrtodactylus aequalis (1)	LSUHC 14060	Kyaiktiyo Hill, Mon State, Myanmar (17.28819°N, 97.05974°E)	MN534914		
Cyrtodactylus aequalis (1)	LSUHC 14065	Kyaiktiyo Hill, Mon State, Myanmar (17.28819°N, 97.05974°E)	MH198647		
Cyrtodactylus cf. aequalis (2)	LSUHC 14242	Kay Lar Tha Hill, Mon State, Myanmar (17.22223°N, 97.09014°E)	MN534905		
Cyrtodactylus cf. aequalis (2)	LSUHC 14244	Kay Lar Tha Hill, Mon State, Myanmar (17.22223°N, 97.09014°E)	MN534906		
Cyrtodactylus cf. aequalis (2)	LSUHC 14243	Kay Lar Tha Hill, Mon State, Myanmar (17.22223°N, 97.09014°E)	MN534907		
Cyrtodactylus cf. aequalis (2)	LSUHC 14245	Kay Lar Tha Hill, Mon State, Myanmar (17.22223°N, 97.09014°E)	MN534908		
Cyrtodactylus bayinnyinensis (3)	LSUHC 13261	Hpa-pu Hill 3.1 km north of Hpa-an, Hpa-an District, Mon State, Myanmar (16.91072°N, 97.62716°E)	MH198651		
Cyrtodactylus bayinnyinensis (3)	LSUHC 13262	Hpa-pu Hill 3.1 km north of Hpa-an, Hpa-an District, Mon State, Myanmar (16.91072°N, 97.62716°E)	MH198650		
Cyrtodactylus bayinnyinensis (3)	LSUHC 13263	Hpa-pu Hill 3.1 km north of Hpa-an, Hpa-an District, Mon State, Myanmar (16.91072°N, 97.62716°E)	MH198649		
Cyrtodactylus bayinnyinensis (3)	LSUHC 13264	Hpa-pu Hill 3.1 km north of Hpa-an, Hpa-an District, Mon State, Myanmar (16.91072°N, 97.62716°E)	MH198648		
Cyrtodactylus bayinnyinensis (4)	LSUHC 13265	Bayin Nyi Cave 16.8 km northwest of Hpa-an, Hpa- an District, Kayin State, Myanmar (16.97048°N, 97.49378°E)	MH198647		
Cyrtodactylus chaunghanakwaensis (5)	LSUHC 13296	Chaunghanakwa Hill 50 km southeast of Mawlamyine, Mawlamyine District, Mon State, Myanmar (16.18456°N, 97.98814°E)	MH198646		
Cyrtodactylus chaunghanakwaensis (5)	LSUHC 13297	Chaunghanakwa Hill 50 km southeast of Mawlamyine, Mawlamyine District, Mon State, Myanmar (16.18456°N, 97.98814°E)	MH198645		
Cyrtodactylus chaunghanakwaensis (5)	LSUHC 13299	Chaunghanakwa Hill 50 km southeast of Mawlamyine, Mawlamyine District, Mon State, Myanmar (16.18456°N, 97.98814°E)	MH198644		
Cyrtodactylus chaunghanakwaensis (5)	LSUHC 13300	Chaunghanakwa Hill 50 km southeast of Mawlamyine, Mawlamyine District, Mon State, Myanmar (16.18456°N, 97.98814°E)	MH198643		
Cyrtodactylus chaunghanakwaensis (5)	LSUHC 13301	Chaunghanakwa Hill 50 km southeast of Mawlamyine, Mawlamyine District, Mon State, Myanmar (16.18456°N, 97.98814°E)	MH198642		
Cyrtodactylus chaunghanakwaensis (5)	LSUHC 13302	Chaunghanakwa Hill 50 km southeast of Mawlamyine, Mawlamyine District, Mon State, Myanmar (16.18456°N, 97.98814°E)	MH198641		
Cyrtodactylus chaunghanakwaensis (5)	LSUHC 13303	Chaunghanakwa Hill 50 km southeast of Mawlamyine, Mawlamyine District, Mon State, Myanmar (16.18456°N, 97.98814°E)	MH198640		

TABLE 1. (Continued)

Taxon	Catalog no.	Locality	GenBank no.		
Cyrtodactylus chaunghanakwaensis (5)	LSUHC 13305	Chaunghanakwa Hill 50 km southeast of Mawlamyine, Mawlamyine District, Mon State, Myanmar (16.18456°N, 97.98814°E)	MH198639		
Cyrtodactylus chaunghanakwaensis (5)	LSUHC 13306	Chaunghanakwa Hill 50 km southeast of Mawlamyine, Mawlamyine District, Mon State, Myanmar (16.18456°N, 97.98814°E)	MH198638		
Cyrtodactylus chaunghanakwaensis (5)	LSUHC 13307	Chaunghanakwa Hill 50 km southeast of Mawlamyine, Mawlamyine District, Mon State, Myanmar (16.18456°N, 97.98814°E)	MH198637		
Cyrtodactylus dammathetensis (6)	LSUHC 12862	Dammathet Cave 19.8 km east of Mawlamyine, Mawlamyine District, Mon State, Myanmar (16.30380°N, 97.48629°E)	MF872276		
Cyrtodactylus dammathetensis (6)	LSUHC 12863	Dammathet Cave 19.8 km east of Mawlamyine, Mawlamyine District, Mon State, Myanmar (16.30380°N, 97.48629°E)	MF872277		
Cyrtodactylus dammathetensis (6)	LSUHC 12864 Dammathet Cave 19.8 km east of Mawlamyine, Mawlamyine District, Mon State, Myanmar (16.30380°N, 97.48629°E)				
Cyrtodactylus dattkyaikensis sp. nov. (7)	LSUHC 14201	Datt Kyaik Cave, Kayin State, Myanmar (17.02854°N, 97.47071°E)	MN534902		
Cyrtodactylus dattkyaikensis sp. nov. (7)	LSUHC 14203	Datt Kyaik Cave, Kayin State, Myanmar (17.02854°N, 97.47071°E)	MN534903		
Cyrtodactylus dattkyaikensis sp. nov. (7)	LSUHC 14204	Datt Kyaik Cave, Kayin State, Myanmar (17.02854°N, 97.47071°E)	MN534904		
Cyrtodactylus naungkayaingensis (8)	LSUHC 13207	Naung Ka Yaing Hill, 17 km north-east of Hpa-an, Hpa-an District, Kayin State, Myanmar (17.01588°N, 97.70641°E)	MH198664		
Cyrtodactylus naungkayaingensis (8)	LSUHC 13208	Naung Ka Yaing Hill, 17 km north-east of Hpa-an, Hpa-an District, Kayin State, Myanmar (17.01588°N, 97.70641°E)	MH198663		
Cyrtodactylus naungkayaingensis (8)	LSUHC 13209	Naung Ka Yaing Hill, 17 km north-east of Hpa-an, Hpa-an District, Kayin State, Myanmar (17.01588°N, 97.70641°E)	MH198662		
Cyrtodactylus sinyineensis (9)	LSUHC 12835	Sin Yine Cave 18.5 km southeast of Hpa-an, Hpa-an District, Kayin State, Myanmar (16.44606°N, 97.29493°E)	MF872354		
Cyrtodactylus sinyineensis (9)	LSUHC 12836	Sin Yine Cave 18.5 km southeast of Hpa-an, Hpa-an District, Kayin State, Myanmar (16.44606°N, 97.29493°E)	MF872355		
Cyrtodactylus sinyineensis (9)	LSUHC 12837	Sin Yine Cave 18.5 km southeast of Hpa-an, Hpa-an District, Kayin State, Myanmar (16.44606°N, 97.29493°E)	MF872356		
Cyrtodactylus sinyineensis (10)	LSUHC 14177	Shwegabin Mountain, Kayin State, Myanmar (16.82407°N 97.66810°E)	MN534923		
Cyrtodactylus sinyineensis (10)	LSUHC 14178	Shwegabin Mountain, Kayin State, Myanmar (16.82210°N, 97.67066°E)	MN534920		
Cyrtodactylus sinyineensis (10)	LSUHC 14179	Shwegabin Mountain, Kayin State, Myanmar (16.82210°N, 97.67066°E)	MN534921		
Cyrtodactylus sinyineensis (10)	LSUHC 14180	Shwegabin Mountain, Kayin State, Myanmar (16.82210°N, 97.67066°E)	MN534922		
Cyrtodactylus sinyineensis (10)	LSUHC 14181	Shwegabin Mountain, Kayin State, Myanmar (16.82210°N, 97.67066°E)	MN534919		
Cyrtodactylus sinyineensis (10)	LSUHC 14182	Shwegabin Mountain, Kayin State, Myanmar (16.82210°N, 97.67066°E)	MN534924		

TABLE 1. (Continued)

Taxon	Catalog no.	Locality	GenBank no.
Cyrtodactylus sinyineensis (11)	LSUHC 13218	Kok Ka Thaung, Kayin State, Myanmar (16.82854°N, 97.70561°E)	MH198661
Cyrtodactylus sinyineensis (11)	LSUHC 13219	Kok Ka Thaung, Kayin State, Myanmar (16.82854°N, 97.70561°E)	MH198660
Cyrtodactylus taungwineensis sp. nov. (12)	LSUHC 14105	Taung Wine Mountain, Kayin State, Myanmar (16.82854°N, 97.70561°E)	MN534931
Cyrtodactylus taungwineensis sp. nov. (12)	LSUHC 14106	Taung Wine Mountain, Kayin State, Myanmar (16.82854°N, 97.70561°E)	MN5349XX
Cyrtodactylus taungwineensis sp. nov. (12)	LSUHC 14109	Taung Wine Mountain, Kayin State, Myanmar (16.82854°N, 97.70561°E)	MN534932
Cyrtodactylus taungwineensis sp. nov. (12)	LSUHC 14117	Taung Wine Mountain, Kayin State, Myanmar (16.82854°N, 97.70561°E)	MN534901
Cyrtodactylus taungwineensis sp. nov. (12)	LSUHC 14110	Taung Wine Mountain, Kayin State, Myanmar (16.82854°N, 97.70561°E)	MN534927
Cyrtodactylus taungwineensis sp. nov. (12)	LSUHC 14114	Taung Wine Mountain, Kayin State, Myanmar (16.82854°N, 97.70561°E)	MN534929
Cyrtodactylus taungwineensis sp. nov. (12)	LSUHC 14107	Taung Wine Mountain, Kayin State, Myanmar (16.82854°N, 97.70561°E)	MN534933
Cyrtodactylus taungwineensis sp. nov. (12)	LSUHC 14108	Taung Wine Mountain, Kayin State, Myanmar (16.82854°N, 97.70561°E)	MN534934
Cyrtodactylus taungwineensis sp. nov. (12)	LSUHC 14113	Taung Wine Mountain, Kayin State, Myanmar (16.82854°N, 97.70561°E)	MN534937
Cyrtodactylus taungwineensis sp. nov. (12)	LSUHC 14112	Taung Wine Mountain, Kayin State, Myanmar (16.82854°N, 97.70561°E)	MN534936
Cyrtodactylus taungwineensis sp. nov. (12)	LSUHC 14111	Taung Wine Mountain, Kayin State, Myanmar (16.82854°N, 97.70561°E)	MN534935
Cyrtodactylus taungwineensis sp. nov. (12)	LSUHC 14115	Taung Wine Mountain, Kayin State, Myanmar (16.82854°N, 97.70561°E)	MN534925
Cyrtodactylus taungwineensis sp. nov. (12)	LSUHC14116	Taung Wine Mountain, Kayin State, Myanmar (16.82854°N, 97.70561°E)	MN534928
Cyrtodactylus taungwineensis sp. nov. (12)	LSUHC_ 14118	Taung Wine Mountain, Kayin State, Myanmar (16.82854°N, 97.70561°E)	MN534930
Cyrtodactylus welpyanensis (13)	LSUHC 12784	Wel Pyan Cave 35 km north of Hpa-an, Hpa-an District, Kayin State, Myanmar (17.1288°N, 97.37066°E)	MF872359
Cyrtodactylus welpyanensis (13)	LSUHC 12785	Wel Pyan Cave 35 km north of Hpa-an, Hpa-an District, Kayin State, Myanmar (17.1288°N, 97.37066°E)	MF872360
Cyrtodactylus welpyanensis (13)	LSUHC 12786	Wel Pyan Cave 35 km north of Hpa-an, Hpa-an District, Kayin State, Myanmar (17.1288°N, 97.37066°E)	MF872361
Cyrtodactylus welpyanensis (13)	LSUHC 12792	Wel Pyan Cave 35 km north of Hpa-an, Hpa-an District, Kayin State, Myanmar (17.1288°N, 97.37066°E)	MF872362

Genomic DNA was isolated from liver or skeletal muscle specimens stored in 95% ethanol using a SPRI magnetic bead extraction protocol (https://github.com/phyletica/lab-protocols/blob/master/extraction-spri.md). The ND2 gene was amplified using a double-stranded Polymerase Chain Reaction (PCR) under the following conditions: 1.0 μ l genomic DNA (10–30 μ g), 1.0 μ l light strand primer (concentration 10 μ M), 1.0 μ l heavy strand primer (concentration 10 μ M), 1.0 μ l dinucleotide pairs (1.5 μ M), 2.0 μ l 5x buffer (1.5 μ M), MgCl 10x buffer (1.5 μ M), 0.1 μ l Taq polymerase (5u/ μ l), and 6.4 μ l ultra-pure H₂O. PCR reactions were executed on Bio-Rad gradient thermocycler under the following conditions: initial denaturation at 95°C for 2 min, followed by a second denaturation at 95°C for 35 s, annealing at 55°C for 35 s, followed by a cycle extension at 72°C for 35 s, for 31 cycles. All PCR products were visualized on a 1.0 % agarose gel electrophoresis. Successful PCR products were sent to GE-

NEWIZ® for PCR purification, cycle sequencing, sequencing purification, and sequencing using the same primers as in the amplification step (Table 2). Sequences were analyzed from both the 3' and the 5' ends separately to confirm congruence between reads. Forward and reverse sequences were uploaded and edited in Geneious™ 2019.0.4 (https://www.geneious.com). Following sequence editing we aligned the protein-coding region and the flanking tRNAs using the MAFTT v7.017 (Katoh & Kuma 2002) plugin under the default settings in Geneious™ 2019.0.4 (https://www.geneious.com). Mesquite v3.04 (Maddison & Maddison 2015) was used to calculate the correct amino acid reading frame and to confirm the lack of premature stop codons in the ND2 portion of the DNA fragment.

TABLE 2. Primer sequences used in this study for amplification and sequencing the ND2 gene and the flanking tRNAs.

Primer name	Primer reference		Sequence
L4437b	(Macey et al. 1997)	External	5'-AAGCAGTTGGGCCCATACC-3'
H5934	(Macey et al. 1997)	External	5' -AGRGTGCCAATGTCTTTGTGRTT-3'

Two model-based phylogenetic analyses were employed. A Maximum Likelihood (ML) analysis was implemented in the IQ-TREE webserver (Nguyen et al. 2015; Trifinopoulos et al. 2016) preceded by the selection of a substitution model using the Bayesian Information Criterion (BIC) in ModelFinder (Kalyaanamoorthy et al. 2017), which supported TVMe+I+G4 as the best fit model of evolution for the tRNAs and TVM+F+I+G4, TIM3+F+I+G4, and GTR+F+ASC+G4 for ND2 codon positions 1-3, respectively. One-thousand bootstrap pseudoreplicates via the ultrafast bootstrap (UFB; Hoang et al. 2018) approximation algorithm were employed and nodes having ML UFB values of 95 and above were considered highly supported (Minh et al. 2013). A Bayesian inference (BI) phylogenetic analysis was carried out in MrBayes 3.2.3. on XSEDE (Ronquist et al. 2012) through CIPRES Science Gateway (Cyberinfrastructure for Phylogenetic Research; Miller *et al.* 2010) employing default priors and HKY + Γ model of evolution for the tRNA and the second codon position and GTR + Γ for the first and third codon positions. Two independent Markov chain Monte Carlo (MCMC) analyses were performed with four chains, three hot and one cold. We ran the MCMC simulation for 150 million generations, sampled every 15 thousand generations and discarded the first 25% of each run as burn-in. Convergence and stationarity of all parameters in the parameter (.p) files from both runs were checked in Tracer v1.6 (Rambaut et al. 2014) to ensure effective sample sizes (ESS) were above 200 for all parameters. Post-burn-in sampled trees from both runs were combined and a 50% majority-rule consensus tree was constructed. Nodes with Bayesian posterior probabilities of 0.95 and above were considered highly supported (Huelsenbeck et al. 2001; Wilcox et al. 2002). After removing outgroup taxa, MEGA7 (Kumar et al. 2016) was used to calculate uncorrected pairwise sequence divergence among the species of the C. sinyineesis group.

Morphological analysis. Color notes and digital images were taken from living specimens prior to preservation. Measurements were taken on the left side of the body when possible to the nearest 0.1 mm using Mitutoyo dial calipers under a Nikon SMZ 1500 dissecting microscope. Measurements following Grismer et al. (2018a,b) were: snout-vent length (SVL), taken from the tip of snout to the vent; tail length (TL), taken from the vent to the tip of the tail, original or regenerated; tail width (TW), taken at the base of the tail immediately posterior to the postcloacal swelling; forearm length (FL), taken on the dorsal surface from the posterior margin of the elbow while flexed 90° to the inflection of the flexed wrist; tibia length (TBL), taken on the ventral surface from the posterior surface of the knee while flexed 90° to the base of the heel; axilla to groin length (AG), taken from the posterior margin of the forelimb at its insertion point on the body to the anterior margin of the hind limb at its insertion point on the body; head length (HL), the distance from the posterior margin of the retroarticular process of the lower jaw to the tip of the snout; head width (HW), measured at the angle of the jaws; head depth (HD), the maximum height of head measured from the occiput to the throat; eye diameter (ED), the greatest horizontal diameter of the eye-ball; eye-to-ear distance (EE), measured from the anterior edge of the ear opening to the posterior edge of the eye-ball; eye to snout distance (ES), measured from anteriormost margin of the eye-ball to the tip of snout; eye-to-nostril distance (EN), measured from the anterior margin of the eye ball to the posterior margin of the external nares; inter orbital distance (IO), measured between the anterior edges of the orbit across the frontal bone; ear diameter (EL), the greatest vertical distance of the ear opening; and internarial distance (IN), measured between the nares across the rostrum.

Meristic characters taken were the numbers of supralabial scales (SL) counted from the largest scale immediately below the middle of the eyeball to the rostral scale and infralabial scales (IL), the large scales counted from the mental scale to the commissure of the jaw. This count was modified from Grismer *et al.* (2018b) whose counts

terminated below the middle of the eyeball. These counts were re-taken for all members of the C. sinyineensis group and used herein in the statistical analyses. Other meristic characters were the number of paravertebral tubercles (PV) between limb insertions counted in a straight line immediately left of the vertebral column; the number of longitudinal rows of body tubercles (LT) counted transversely across the center of the dorsum from one ventrolateral fold to the other; the number of longitudinal rows of ventral scales (VS) counted transversely across the center of the abdomen from one ventrolateral fold to the other; the number of expanded subdigital lamellae proximal to the digital inflection on the fourth toe (ET4) counted from the base of the first phalanx where it contacts the body of the foot to the largest scale on the digital inflection (see Grismer et al. 2018a: Fig. 3), large continuous scales on the palmar and plantar surfaces were not counted; the number of small, unmodified subdigital lamellae distal to the digital inflection to the claw including the claw sheath on the fourth toe (UT4) counted from the digital inflection to the claw (see Grismer et al. 2018a: Fig. 3); and the total number of subdigital lamellae (TT4) beneath the fourth toe (i.e. ET4 + UT4 = TT4). The total number of enlarged femoral scales (FS) from each thigh were combined as a single metric. The total number of femoral pores (FP) in males (i.e., the sum of the number of enlarged pore-bearing femoral scales from each leg combined as a single metric—not all enlarged femoral scales have pores). The number of enlarged precloacal scales (PS); the number of precloacal pores in (PP) in males; and the number of rows of post-precloacal scales (PPS) on the midline between the enlarged precloacal scales and the vent (see Grismer et al. 2018a:Fig. 4); number of dark body bands (BB) between the occiput and the hind limb insertions not including the sacral or postsacral bands; the number of light-colored caudal bands on an original tail; the number of dark caudal bands on an original tail; and if a mature regenerated tail was spotted or not.

Non-meristic morphological characters evaluated were the degree of body tuberculation—weak tuberculation referring to dorsal body tubercles that are relatively low, small, less densely packed, and weakly keeled whereas prominent tuberculation refers to tubercles that are larger, higher (raised), and prominently keeled (see Grismer *et al.* 2018a: Fig. 6); body tubercles extending past the postcloacal swelling or not (see Grismer *et al.* 2018a: Fig. 7); and the relative length-to-width ratio of the transversely expanded, median subcaudal scales and whether or not they extend onto the lateral surface of the tail (see Grismer *et al.* 2018a: Fig. 8).

Color pattern characters (see Grismer *et al.* 2018a: Fig. 5) evaluated were the nuchal loop being continuous from eye to eye, separated medially into paravertebral halves, bearing an anterior azygous notch or not, and the posterior border being straight (smooth), sinuous, v-shaped, jagged, or having two posteriorly directed projections; dorsal body bands bearing paired, paravertebral elements or not; dark dorsal body bands wider than light interspaces, with or without lightened centers, edged with light-colored tubercles or not, jagged or more regularly shaped (straight or even-edged); dark markings present or absent in the dorsal interspaces; top of head bearing combinations of dark diffuse mottling or dark, distinct blotches overlain with a light-colored reticulating network or not; light caudal bands bearing dark markings or immaculate; light caudal bands encircle tail or not; dark caudal bands wider than light caudal bands; and regenerated tail bearing a pattern of distinct, dark spots or not.

All statistical analyses were performed using the platform R v 3.2.1 (R Core Team 2018). A multivariate analysis of variance (MANOVA) using Pillai lamda was conducted to ascertain if the population/lineage pairs delimited in the molecular phylogenies were significantly different (p < 0.05) in multivariate morphological space. Morphospatial positions were subsequently visualized using principal component analysis (PCA) from the ADEGENET package in R (Jombart et al. 2010) to determine if their positioning was consistent with the putative species boundaries delimited by the molecular phylogenetic analyses and defined by the univariate analyses (see below). PCA, implemented by the prcomp() command in R, is an indiscriminate analysis plotting the overall variation among individuals (i.e. data points) while treating each individual independently (i.e. not coercing data points into pre-defined groups). Meristic data used were SL, IL, PV, LT, VS, ET4, UT4, TT4, FS, PS, and PPS. Femoral and precloacal pore counts were excluded from the PCA due to their absence in females. Because the data were skewed by values ranging from 3–36, all characters were scaled to their standard deviation prior to analysis in order to normalize their distribution so as to ensure characters with very large and very low values did not over-leverage the results owing to intervariable nonlinearity and to ensure the data were analyzed on the basis of correlation not covariance. Based on the PCA, a discriminant analysis of principle components (DAPC) was performed which places the individuals of each predefined population inferred from the phylogeny into separate clusters (i.e., plots of points) bearing the smallest within-group variance that produce linear combinations of centroids having the greatest between-group variance (i.e. linear distance; Jombart et al. 2010). DAPC relies on standardized data from a PCA as a prior step to ensure that variables analyzed are not correlated and number fewer than the sample size. DAPC principal components with eigenvalues accounting for 90–99% of the variation in the data set were retained for the DAPC analysis according to the criterion of Jombart *et al.* (2010).

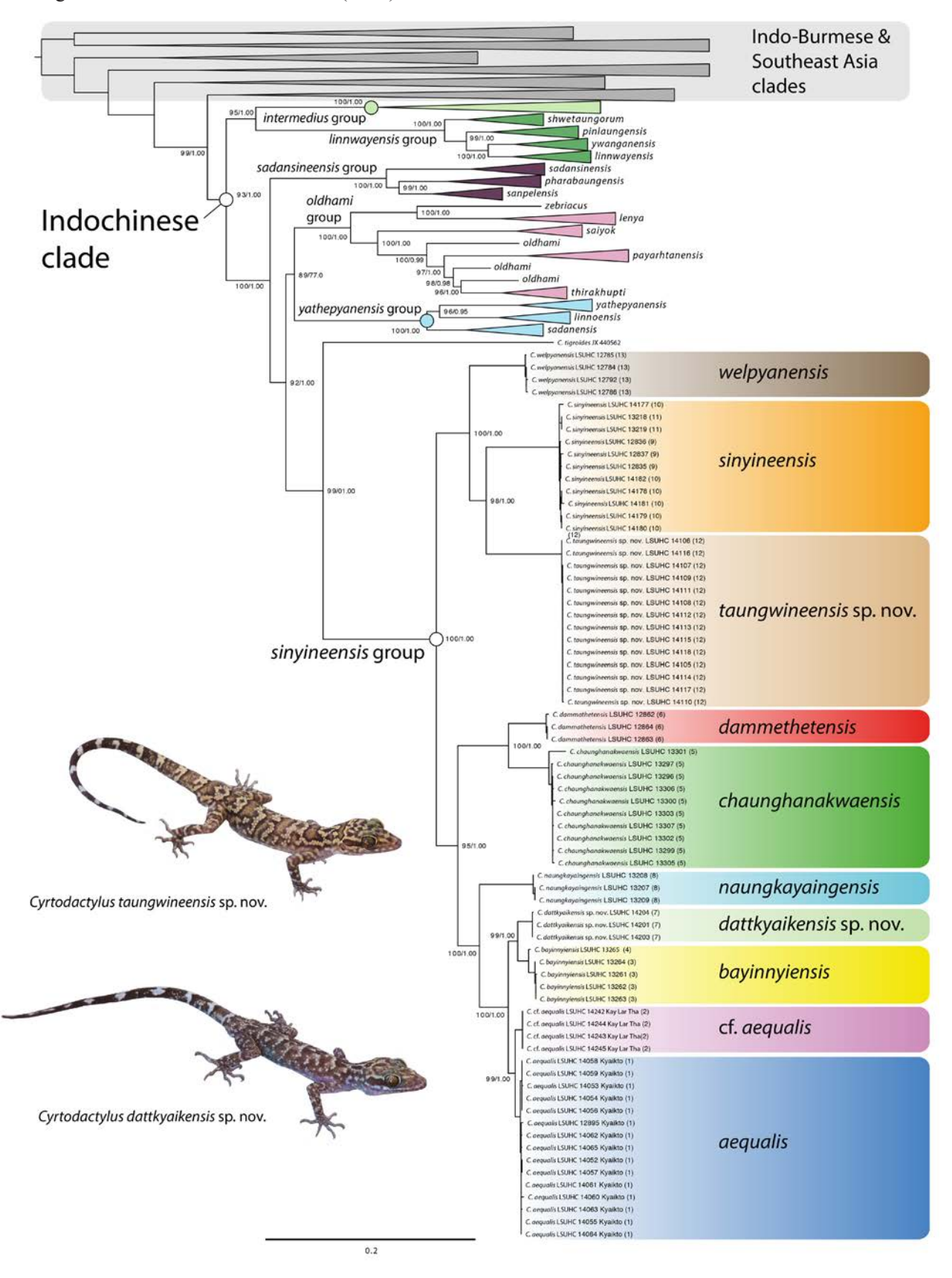


FIGURE 3. Majority-rule consensus tree from the ML bootstrap replicates of the Indochinese clade with UFB and BI support values, respectively, at the nodes.

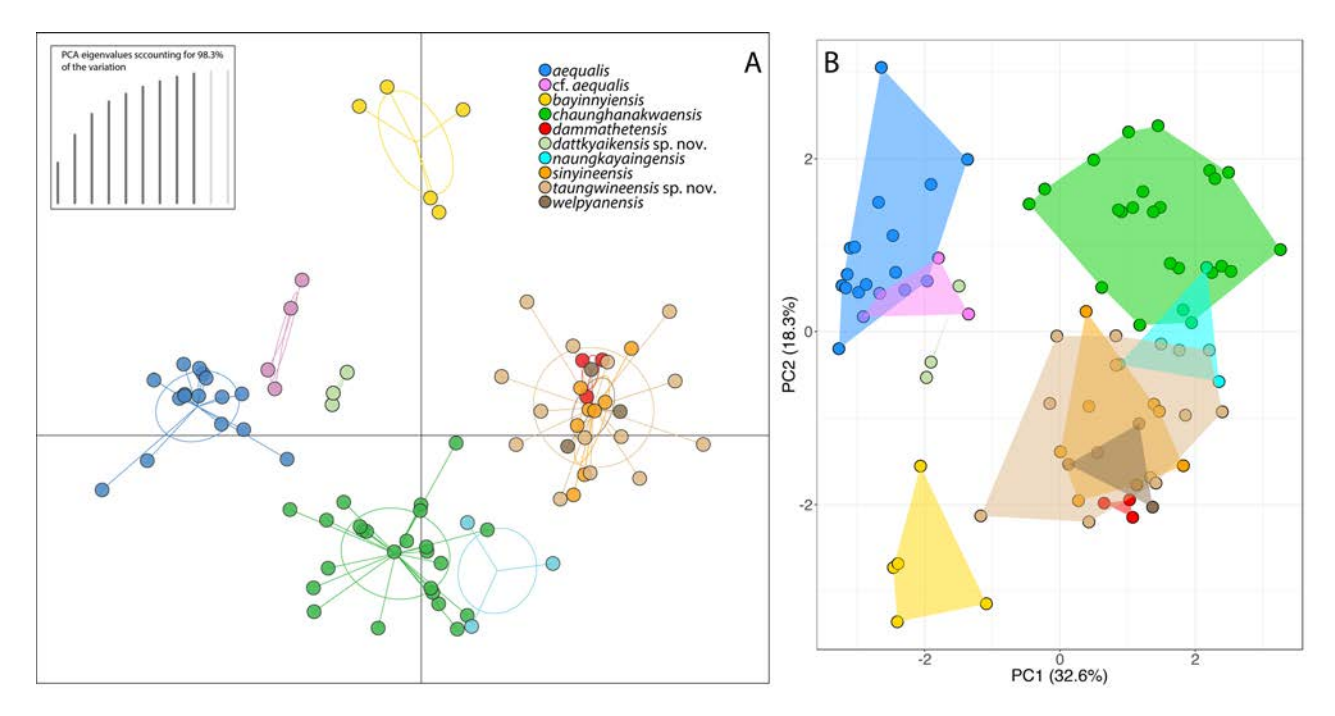


FIGURE 4. A. Plot of the discriminant analysis of principal components (DAPC). B. Plot of the principal component analysis (PCA) ordinated along the first two principal components.

Independent of the MANOVA, an analysis of variance (ANOVA) was conducted on characters with similar variances (*i.e.*, p > 0.05 in a Levene's test) to test for the presence of statistically significant mean differences (p < 0.05) in the data set. Characters bearing statistical differences across the data set were subjected to a TukeyHSD test to ascertain which population pairs differed significantly from each other for the means of those characters. Boxplots were generated using custom R script in order to visualize the range and degree of differences between pairs of species bearing statistically significant means values for sets of characters.

Museum abbreviations follow Sabaj (2016) except for LSUHC referring to the La Sierra University Herpetological Collection, La Sierra University, Riverside, California, 92505, USA.

Results

The BI and ML analyses recovered trees with nearly identical topologies based on 1041 parsimony informative sites and indicated that the populations from Datt Kyaik Hill and Taung Wine Hill each formed monophyletic mitochondrial lineages (Fig. 3). The former was recovered as the sister lineage to *Cyrodactylus bayinnyiensis* (UFB 99/BI 1.00) and the latter was most closely related to *C. sinyineensis* (98/1.00). The overall topology of the *C. sinyineensis* group phylogeny matched that of Grismer *et al.* (2018b) where all other nodes relating species were strongly supported ($\geq 95/0.95$).

The MANOVA indicated highly significant morphospatial differences existed within the data set (MANOVA, Pillai, $p = 2.2^{-16}$) as visualized in the PCA (Fig. 4). The first three principal components (PC) were responsible for 64.2% of the variation in the data set (Table 3). PC1 accounted for 32.6% of the variation and loaded most heavily for total number of fourth toe lamellae (TT4), PC2 accounted for 18.2% of the variation, loading most heavily for precloacal scales (PS), and PC3 (not shown) accounted for an additional 13.3% of the variation and loaded most heavily for paravertebral tubercles (PV) and post-precloacal scales (PPS). In the combined ordination of the first two PCs, individuals of the Datt Kyaik Hill population clustered separately from all other species in the *Cyrtodactylus sinyieensis* group except for *C*. cf. *aequalis* although the ANOVA and TukeyHSD (Table 4) indicated they differed significantly in their mean values of expanded fourth toe lamellae (ET4), enlarged precloacal scales (PS), and paravertebral tubercles (PV). Additionally, the phylogeny indicates they are not sister species (Fig. 3). Individuals

TABLE 3. Summary statistics and principal component analysis scores for the species of the *Cyrtodactylus sinyineensis* group. Abbreviations are listed in the Materials and methods.

	PC1	PC2	PC3	PC4	PC5	PC6	PC7	PC8	PC9	PC10	PC11
Standard Deviation	1.88319	1.34959	1.16043	1.07625	0.95920	0.78694	0.75892	0.64686	0.60150	0.48054	0.02892
Proportion of Variance	0.3224	0.16558	0.12242	0.1053	0.08364	0.0563	0.05236	0.03804	0.03289	0.02099	8.00E-05
Cumulative Proportion	0.3224	0.48798	0.6104	0.7157	0.79934	0.85564	0.908	0.94604	0.97893	0.99992	1.00000
Eigenvalue	3.54640	1.82139	1.34659	1.15831	0.92007	0.61927	0.57597	0.41843	0.36181	0.23092	0.00084
SL	0.36663	0.21133	-0.14691	0.14348	-0.27490	0.62820	-0.05058	-0.08091	0.11658	-0.53462	-0.00590
IL	0.40648	0.22580	0.01132	0.14082	-0.33554	0.16416	0.07749	0.26967	-0.36998	0.63919	0.01080
PV	0.05434	0.58841	0.26323	-0.07996	0.07365	-0.05951	-0.43228	-0.49595	0.27204	0.24345	0.00788
LT	-0.26662	0.36894	-0.41997	-0.15593	-0.09179	-0.00683	-0.00988	0.54627	0.52285	0.10808	-0.00847
VS	0.28303	-0.25442	0.03876	-0.52788	0.13594	0.28773	0.44124	-0.20879	0.39278	0.28490	0.00057
ET4	-0.33031	-0.15587	0.47240	-0.02806	0.12693	0.52398	-0.27453	0.29494	0.01365	0.10460	0.42249
UT4	-0.40969	0.17343	-0.09491	0.01784	-0.43338	-0.01368	0.43042	-0.36209	-0.08646	0.01462	0.52980
TT4	-0.47891	0.03671	0.20914	0.00195	-0.23918	0.28977	0.14870	-0.10051	-0.06210	0.08833	-0.73519
FS	0.18726	0.01531	0.61946	0.28339	-0.27506	-0.30793	0.28840	0.22246	0.41842	-0.14980	-0.00156
PS	-0.04942	0.34983	-0.00496	0.44222	0.65989	0.17094	0.46103	0.00924	-0.03393	0.03356	0.00100
PPS	0.04895	0.42301	0.26732	-0.61093	0.08525	-0.09635	0.17697	0.23449	-0.40015	-0.33313	-0.00454

TABLE 4. Pairwise combinations among *Cyrtodactyluys dattkyaikensis* **sp. nov.** and *C. taungwineensis* **sp. nov.** of characters bearing statistically different mean values based on the ANOVA and TunkeyHSD tests between them and all other species of the *C. sinyineensis* group.

	C. dattkyaikensis sp. nov.	C. taungwineensis sp. nov.
C. aequalis	LT, PS	ET4, IL, LT, PV, SL, TT4, UT4, VS
C. cf. aequalis	ET4, PS, PV	TT4, UT4, VS
C. bayinnyiensis	PPS, PS, PV	ET4, PPS, PV, TT4, VS
C. chaunghanakwaensis	ET4, IL, PS, TT4	FS, IL, PS, PV, VS
C. dammethetensis	FS, IL, LT, PS	ET4, FS, LT, VS
C. naungkayaingensis	ET4, PS, TT4	FS, PV, VS
C. sinyineensis	IL, VS	ET4, FS, PV
C. taungwineensis sp. nov.	ET4, PS, TT4, VS	
C. welpyanensis	FS, PS	FS, LT

TABLE 5. Uncorrected pairwise sequence divergences between the mitochondrial ND2 lineages of the *Cyrtodactylus sinyineensis* group. Bold values are intralineage values.

	1	2	3	4	5	6	7	8	9	10
1. C. aequalis K	0.002									
2. C. cf. aequalis KLT	0.011	0.000								
3. C. byainnyiensis	0.030	0.031	0.004							
4. C. chaunghanakwaensis	0.101	0.101	0.105	0.003						
5. C. dammathetensis	0.097	0.096	0.097	0.061	0.002					
6. C. dattkyaikensis sp. nov.	0.031	0.032	0.023	0.108	0.102	0.000				
7. C. naungkayaingensis	0.071	0.070	0.072	0.109	0.099	0.074	0.001			
8. C. sinyineensis	0.123	0.126	0.125	0.144	0.136	0.130	0.123	0.004		
9. C. taungwinenesis sp. nov.	0.115	0.118	0.117	0.132	0.130	0.125	0.125	0.099	0.000	
10. C. welpyanensis	0.104	0.104	0.112	0.120	0.114	0.112	0.106	0.093	0.093	0.002

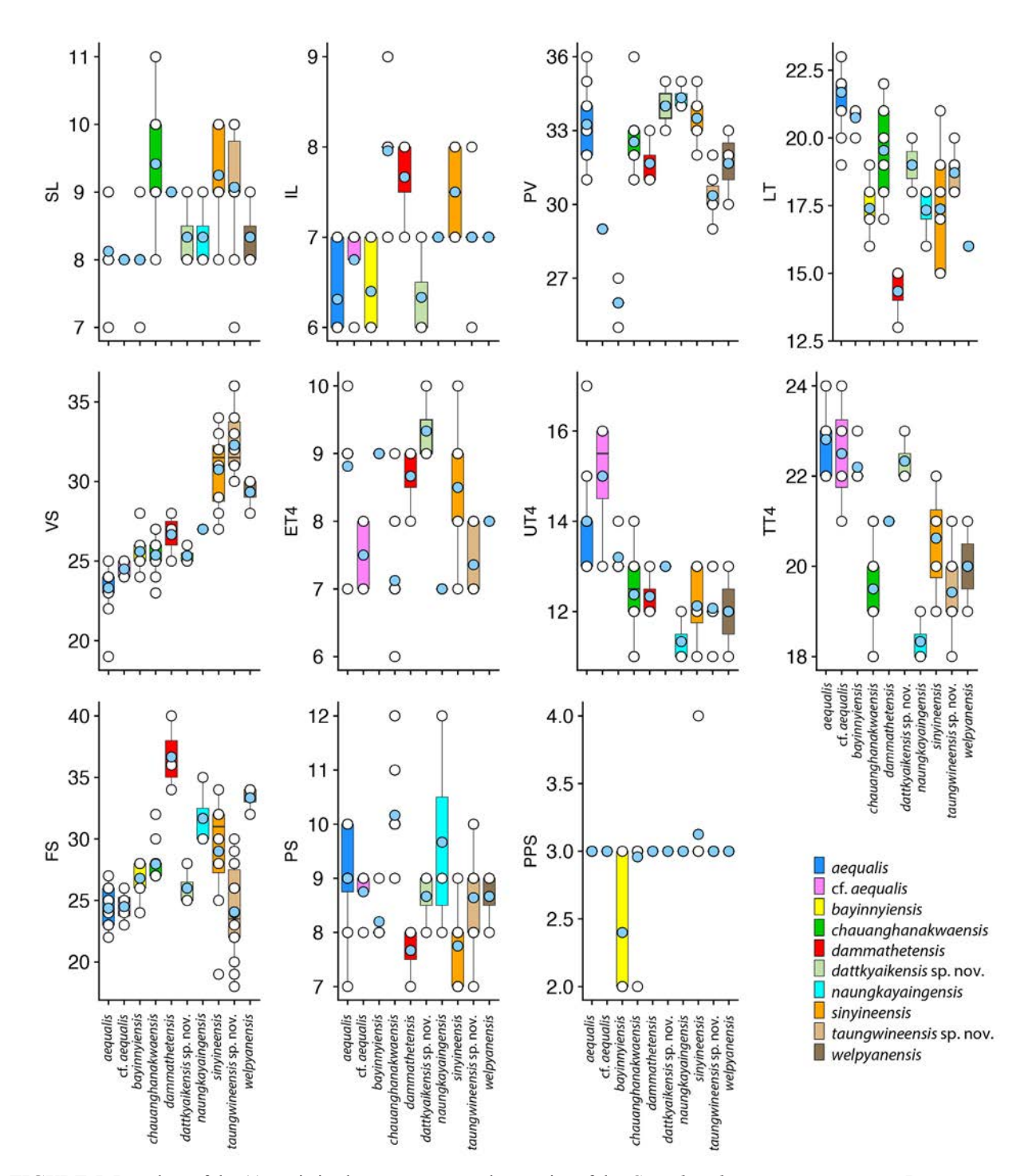


FIGURE 5. Boxplots of the 11 meristic characters among the species of the *Cyrtodactylus sinyineensis* group. Boxes represent the 50% quartiles, the horizontal black bars the medians, and the light-blue circles the means. Boxes are absent for certain characters for some species because those characters do not vary. Abbreviations are in the Materials and Methods.

from the Taung Wine Hill population clustered separately from all other species except for *C. dammathetensis*, *C. naungkayaingensis*, *C. sinyineensis*, and *C. welpyanensis* and the ANOVA and TukeyHSD indicated it differs significantly from these three species across a range of characters (Fig. 5, Table 4). The lineages of the clade composed of *C. aequalis*, *C. bayinnyiensis*, and the Datt Kyaik Hill population, completely overlap one another along PC1 and are nearly completely separated along PC2. The clade composed of the lineages *C. sinyineensis*, *C. welpyanensis*, and the Taung Wine Hill population completely overlap one another along PC1 and PC2 and in the DAPC—demonstrating their overall similarity in squamation despite being separate phylogenetic lineages bearing a 9.3–9.9% uncorrected pairwise sequence divergence among them (Table 5). *Cyrtodactylus aequalis*, *C.* cf. *aequalis*,

C. bayinyiensis, *C. chanhanakwaensis*, *C. naungkayaingensis*, and the Datt Kyaik Hill population do not overlap any members of the *C. sinyineensis* group in the DAPC (Fig. 4). The ANOVA and TukeyHSD analyses indicate that the Datt Kyaik Hill and Taung Wine Hill populations differ statistically from each other and all other species in the *C. sinyineensis* group across a broad range of characters (Fig. 5, Table 4). Given the corroboration of the genetic and morphological data, we construct robust and testable hypotheses below by describing the Datt Kyaik Hill and Taung Wine Hill populations as new species.

Taxonomy

The populations from Datt Kyaik Hill and Taung Wine Hill can be placed in the *Cyrtodactylus sinyineensis* group as revised here from Grismer *et al.* (2018a) by having 8–10 supralabials; 6–8 infralabials; raised, moderately to strongly keeled, dorsal body tubercles that usually extend beyond base of tail; 30–36 paravertebral tubercles; 13–19 longitudinal rows of body tubercles; 19–30 ventral scales; 19–22 total subdigital lamellae; continuous enlarged femoral and precloacal scales; 25–36 similarly sized enlarged femoral scales; 13–36 femoral and 4–9 precloacal pores in males; 5–13 enlarged precloacal scales; three post-precloacal scale rows; transverse, median subcaudal scales usually twice as wide as long, not extending onto lateral surface of tail; top of head bearing dark mottled pattern; no anterior, azygous notch in nuchal loop; five or six variably shaped body bands; anterodorsal margins of thighs and brachia darkly pigmented; 9–11 light-colored caudal bands; 9–11 dark-colored caudal bands; and maximum SVL 69.3–91.6 mm (Grismer *et al.* 2018a).

Cyrotodactylus dattkyaikensis sp. nov.

Datt Kyaik Hill Bent-toed Gecko (Figs. 6, 7, 8)



FIGURE 6. Type series of *Cyrtodactylus dattkyaikensis* **sp. nov.** from Datt Kyaik Hill, Kayin State, Myanmar. LSUHC 14201 is the adult male holotype. LSUHC 14202 and 14203 are the adult male and female paratypes, respectively.

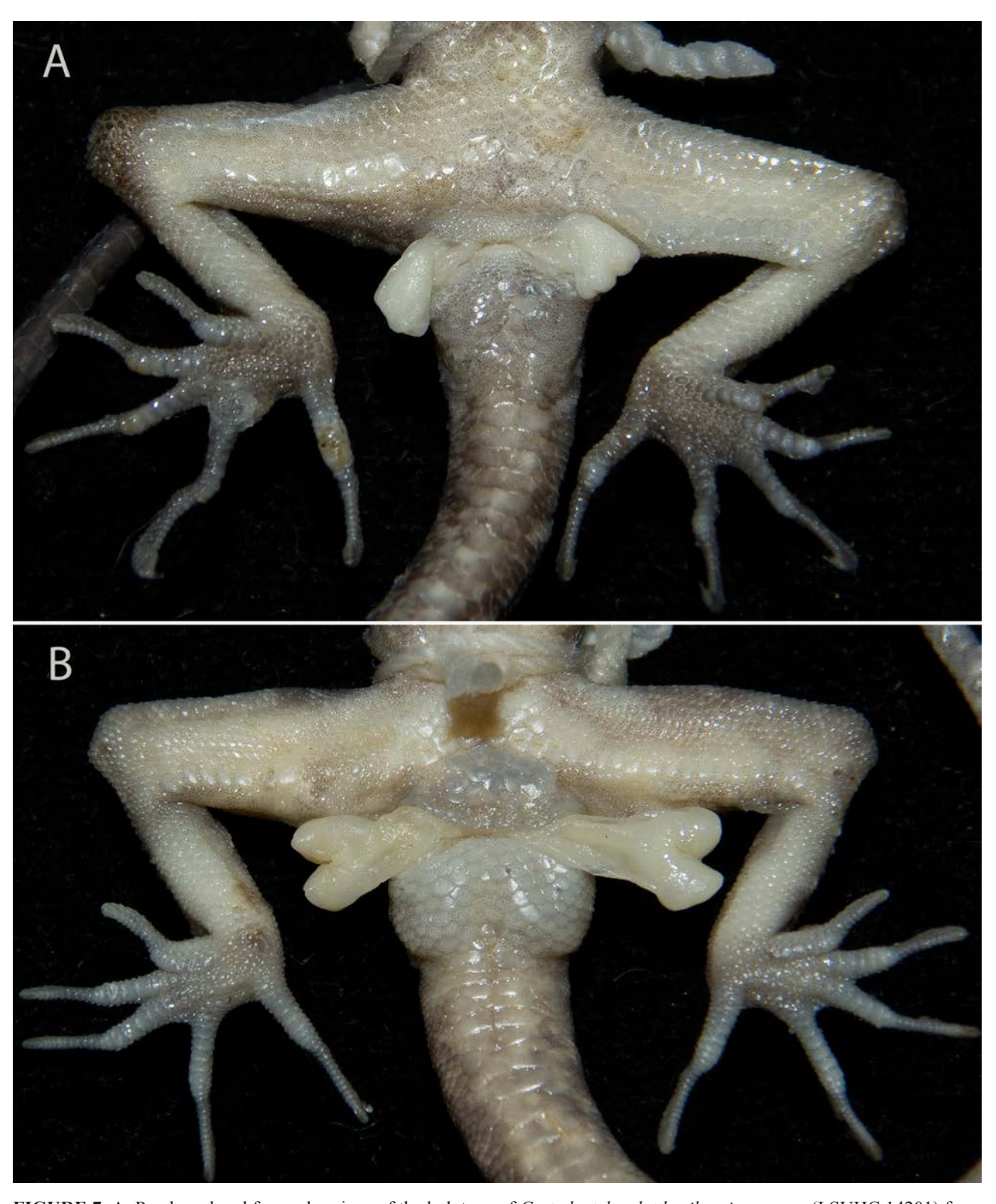


FIGURE 7. A. Precloacal and femoral regions of the holotype of *Cyrtodactylus dattkyaikensis* **sp. nov.** (LSUHC 14201) from Datt Kyaik Hill, Kayin State, Myanmar. B. Precloacal and femoral regions of the holotype of *Cyrtodactylus taungwineensis* **sp. nov.** (LSUHC 14101) from Taung Wine Hill, Kayin State, Myanmar.

Holotype. Adult male LSUHC 14201 was collected on 9 November 2018 at 2000 hrs by Evan S. H. Quah, Myint Kyaw Thura, Jamie R. Oaks, Perry L. Wood Jr., Aung Lin, and L. Lee Grismer from Datt Kyaik Hill, Mon State, 23 km northwest of Hpa-an, Mon State, Myanmar (17.02854°N, 97.47071°E; 12 m in elevation).

Paratypes. Adult male LSUHC 14202 and adult female 14203 bear the same collection data as the holotype.

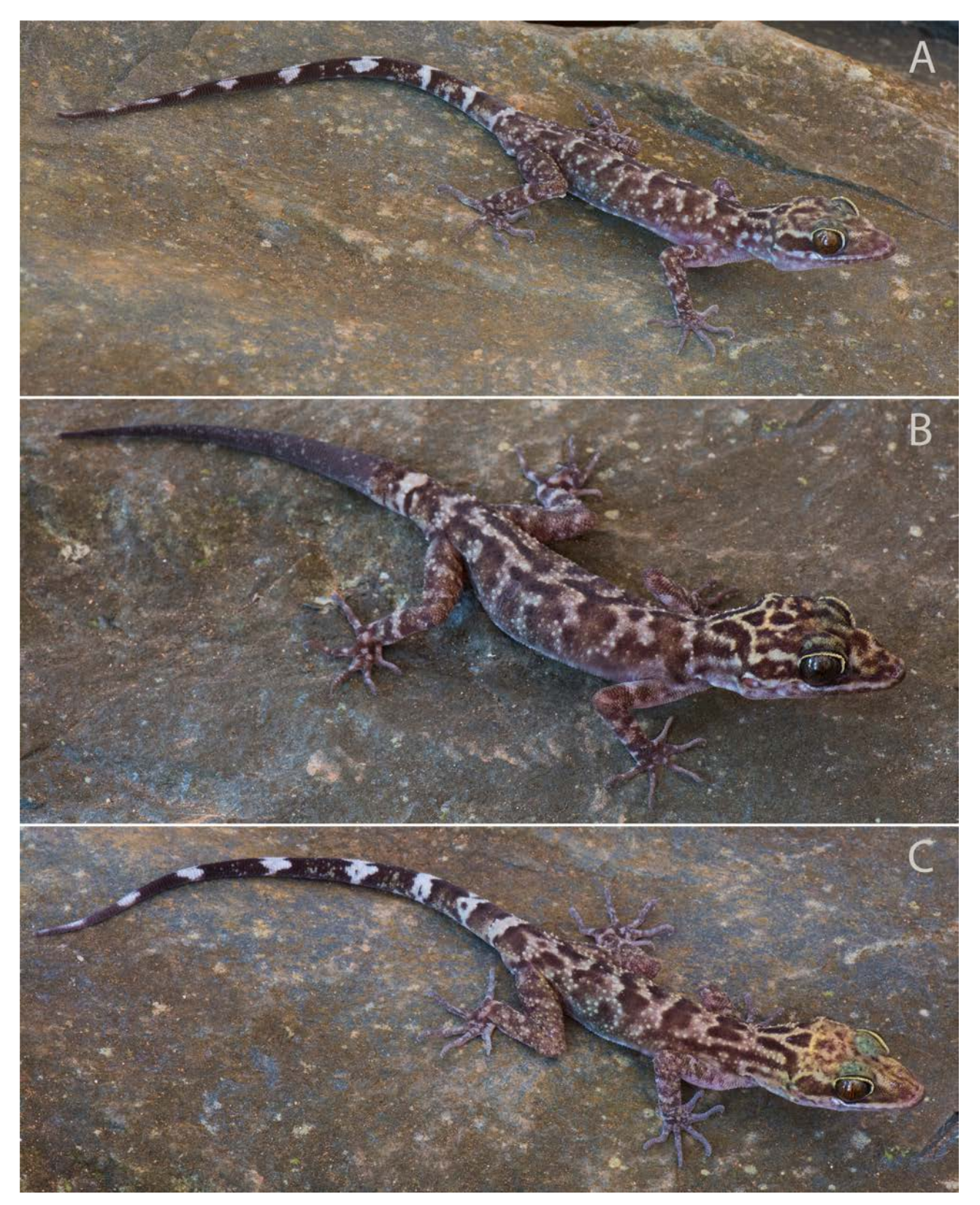


FIGURE 8. Coloration in life of type series of *Cyrtodactylus dattkyaikensis* **sp. nov.** A. Adult male holotype LSUHC 14201. B. Adult female paratype 14203 C. Adult male paratype14202. Photographs by L. Grismer.

Diagnosis. Cyrtodactylus dattkyaikensis **sp. nov.** differs from all species in the *C. sinyineensis* group by having the combination of eight or nine supralabials; six or seven infralabials; 33–35 paravertebral tubercles; 18–20 longitudinal rows of dorsal tubercles; 25 or 26 ventral scales; nine or 10 expanded subdigital lamellae on the fourth

toe; 13 unexpanded subdigital lamellae on the fourth toe; 22 or 23 total subdigital lamellae on the fourth toe; 25–28 enlarged femoral scales; 15 pore-bearing femoral scales in males; eight or nine enlarged precloacal scales; 6–8 pore-bearing precloacal scales in males; three rows of enlarged post-precloacal scales; six dorsal body bands; 7–9 light-colored caudal bands; eight or nine dark-colored caudal bands; raised and strongly keeled dorsal tubercles that extend beyond the postcloacal swelling; enlarged femoral and precloacal scales nearly the same size and continuous; pore-bearing femoral and precloacal scales not continuous; medial subcaudals two to three times wider than long and extending onto lateral side of tail; nuchal loop divided medially, lacking an anterior azygous notch, and bearing a protracted posterior border; no band on nape; some dorsal bands bearing paravertebral elements, wider than interspaces, bearing lightened centers, partly edged with white tubercles, and zig-zag in shape; dark markings in dorsal interspaces; light-colored caudal bands in adults bearing dark-colored markings; light-colored caudal bands not encircling tail; and mature regenerated tail not spotted (Table 6).

TABLE 6. Summary statistics and diagnostic characters of the new species from the *Cyrtodactylus sinyineensis* species groups. SD = standard deviation, n = sample size.

-F - S - S - S - S - S - S - S - S - S -		.,	- xP							
	datikyaikensis sp. nov	taungwineensis sp. nov.	dammathetensis	aequalis	cf. aequalis	sinyineensis	welpyanensis	bayinnyiensis	chaunghanakwaensis	naungkayaingensis
supralabial scales (SL)										
mean (±SD)	8.3 (±0.58)	9.1 (±7– 10)	9.0 (±0.00)	8.1 (±0.50)	8.0 (±0.00)	9.7 (±xx)	8.3 (±0.6)	8.0 (±0.84)	9.4 (±0.71)	8.3 (±0.58)
Range	8 or 9	7–10	9	7–9	8	xxx	8 or 9	7–9	8-11	8 or 9
n	3	14	3	16	4	xx	3	5	24	3
infralabial scales (IL)										
Mean (±SD)	6.3 (±0.57)	7.00 (±0.39)	7.7 (±0.58)	6.3 (±0.48)	6.75 (±0.50)	8	7.0 (±0.00)	6.2 (±0.44)	7.9 (±0.50)	7.0 (±0.00)
Range	6 or 7	6–8	7 or 8	6 or 7	6 or 7	8	7	6 or 7	7–9	7
n	3	14	3	16	4	3	3	5	24	3
paravertebral tubercles (PV)										
Mean (±SD)	34. 0 (±0.00)	30.3 (±0.84)	31.7 (±1.15)	33.3 (±1.44)	29.0 (±0.00)	33.7	31.7 (±1.5)	26.0 (±0.71)	32.5 (±0.98)	34.3 (±0.58)
Range	33–35	29-32	31–33	31–36	29	33–35	30-33	25–27	31–36	34 or 35
n	3	14	3	16	4	3	3	5	24	3
longitudunal rows of body tubercles (LT)										
Mean (±SD)	19.0 (±1.00)	18.7 (±0.61)	14.3 (±1.15)	21.7 (±1.08)	20.8 (±0.50)	15	16.0 (±0.00)	17.4 (±01.14)	19.5 (±1.47)	17.3 (±1.54)
Range	18-20	18-20	13-15	19–23	20 or 21	15	16	16–19	17–22	16-18
n	3	14	3	16	4	3	3	5	24	3
ventral scales (VS)										
Mean (±SD)	25.3 (±0.58)	32.3 (±2.02)	26.7 (±1.53)	23.3 (±1.40)	24.5 (±0.58)	28 (±1.0)	29.3 (±1.20)	25.6 (±1.52)	25.4 (±1.10)	27.0 (±0.00)
Range	25 or 26	30–36	25–28	19–25	24 or 25	27–29	28-30	24–28	23–27	27
n	3	14	3	16	4	3	3	5	24	3
expanded 4th toe lamellae (ET4)										

	datikyaikensis sp. nov	taungwineensis sp. nov.	dammathetensis	aequalis	cf. aequalis	sinyineensis	welpyanensis	bayinnyiensis	chaunghanakwaensis	naungkayaingensis
Mean (±SD)	9.3 (±0.58)	7.4 (·0.50)	8.7 (±0.58)	8.8 (±0.75)	7.5 (±0.58)	9	8.0 (±0.00)	9.0 (±0.00)	7.1 (±0.61)	7. 0 (±0.00)
Range	9 or 10	7 or 8	8 or 9	7–10	7 or 8	8–10	8	9	6–9	7
n	3	14	3	16	4	3	3	5	24	3
unmodified 4th toe lamellae (UT4)										
Mean (±SD)	13.0 (±0.00)	12.1 (±0.62)	12.3 (±0.58)	14.0 (±1.03)	15. 0 (±1.41)	11.3 (±0.58)	12.0 (±1.0)	13.3 (±0.50)	12.4 (±0.92)	11.3 (±0.58)
Range	13	11–13	12 or 13	13-17	13–16	11 or 12	11-13	13 or 14	11-14	11 or 12
n	3	14	3	16	4	3	3	5	24	3
total 4th toe lamellae (TT4)										
Mean (±SD)	23.3 (±0.58)	19.4 (±0.85)	21.0 (±0.00)	22.8 (±0.66)	22.5 (±1.29)	20.3 (±1.6)	20.0 (±1.0)	22.3 (±0.50)	19.5 (±1.06)	18.3 (±0.58)
Range	22 or 23	18-21	21	22-24	21–24	19–21	19–21	22 or 23	18-21	18 or 19
n	3	14	3	16	4	3	3	5	24	3
enlarged femoral scales (FS)										
Mean (±SD)	26.0 (±1.7)	24.1 (±3.83)	33.0 (±2.65)	24.4 (±1.50)	24.5 (±1.29)	26.3 (±0.58)	30.3 (±0.58)	26.8 (±1.79)	28.0 (±1.06)	31.7 (±2.89)
Range	25–28	18-30	31–36	22–27	23–26	26 or 27	30-31	24–28	27–32	30–35
n	3	14	3	16	4	3	3	5	24	3
femoral pores (FP)										
	25.0	16.3	36.0	14.4	/	16	20.0	15.0	28.6	11.0
Mean (±SD)	(±0.00)	(±3.15)	(±0.00)	(±2.94)	,		(±0.00)	(±0.00)	(±1.51)	(±0.00)
Range	25	13–22	36	10–19	/	16	20	15	27–32	11
n enlarged precloacal scales (PS)	2	7	1	7	/	1	2	1	9	2
Mean (±SD)	8.3 (±0.58)	8.6 (±0.84)	8.3 (±0.58)	9.0 (±0.89)	8.8 (±0.50)	11(±1.0)	12.0 (±1.0)	8.2 (±0.45)	10.2 (±0.70)	9.7 (±0.2.08)
Range	8 or 9	7–10	8 or 9	7-10	8 or 9)	10-12	11-13	8 or 9	9-12	8-12
n	3	14	3	16	4	3	3	5	24	3
precloacal pores (PP)										
Mean (±SD)	7.0 (±1.41)	6.6 (±0.79)	9.0 (±0.00)	7.4 (±2.07)	/	5	7.5 (±0.5)	9.0 (±0.00)	9.9 (±0.60)	3.5 (±0.5)
Range	6–8	6–8	9	5-10	/	5	7 or 8	9	9–11	3 or 4
n	2	7	1	7	/	1	2	1	9	2
post-precloacal scale rows (PPS)										
Mean (±SD)	3.0 (±0.00)	3.0 (±0.00)	3.0 (±0.00)	3.0 (±0.00)	3.0 (±0.00)	3	3.0 (±0.00)	2.4 (±0.54)	3.0 ±0.21)	3. 0 (±0.00)

TABLE 6. (Continued)

	dattkyaikensis sp. nov	taungwineensis sp. nov.	dammathetensis	aequalis	cf. aequalis	sinyineensis	welpyanensis	bayinnyiensis	chaunghanakwaensis	naungkayaingensis
Range	3	3	3	3	3	3	3	2 or 3	2 or 3	3
n	3	3	3	16	4	3	3	5	24	3
body bands (BB)										
Mean (±SD)	6.0 (±0.00)	4.1 (±0.26)	5.0 (±0.00)	5.3 (±1.00)	/	5.5 (±0.71)	6.0 (±0.00)	5.2 (±0.83)	5.92 (±0.41)	4.0 (±0.00)
Range	6	4 or 5	5	5–7	/	5 or 6	6	4–6	5–7	4
n	3	14	3	12	/	2	3	5	24	3
light caudal bands (LCB)										
Mean (±SD)	8.0 (±1.41)	12.1 (±0.60)	10.3 (±0.71)	9.6 (±0.52)	/	9	9.0 (±0.00)	9.3 (±2.08)	12.3 (±1.37)	11.0 (±0.00)
Range	7–9	11-13	10 or 11	9 to 10	/	9	9	7–11	10-14	11
n	2	9	3	8	/	1	1	3	6	1
dark caudal bands (DCB)										
Mean (±SD)	8.5 (±0.71)	12.0 (±0.71)	10.7 (±0.71)	9.5 (±0.76)	/	9	10.0 (±0.00)	10.3 (±2.08)	12.7 (±1.37)	10.0 (±0.00)
Range	8 or 9	11-13	10 or 11	9-11	/	9	10	8-12	11-15	10
n	2	9	3	8	/	1	1	3	6	1
Morphology										
Body tubercles low, weakly keeled	no	no	no	no	no	no	no	yes/no	yes	no
body tubercles raised, moderately to strongly keeked	yes	yes	yes	yes	yes	yes	yes	yes/no	no	yes
pore-bearing femoral and precloacal scales continuous	no	no	yes	no	/	no	no	no	yes	no
enlarged proximal femoral scales ~1/2 size of distal femorals	no	no	yes	no	no	no	no	no	no	no
medial subcaudals extend onto lateral surface of tail	yes	no	yes	no	no	no	no	yes	yes	yes
Color Pattern										
nuchal loop divided medially	yes	no	variable	yes	variable	no	no	no	no	no
posterior border of nuchal loop	protracted	protracted	jagged	smooth	smooth	jagged	jagged	jagged	jagged	jagged
band on nape	no	no	yes	yes	no	yes	yes	yes	yes	variable
dorsal banding with paravertebral elements	no	no	yes	yes	no	no	no	variable	yes	yes
dorsal bands wider than interspaces	yes	yes	yes	yes	equal to	yes	yes	yes/no	yes	no

	dattkyaikensis sp. nov	taungwineensis sp. nov.	dammathetensis	aequalis	cf. aequalis	sinyineensis	welpyanensis	bayinnyiensis	chaunghanakwaensis	naungkayaingensis
dorsal bands bearing lightened centers	yes	yes	no	no	yes	weak	no	yes/no	variable	yes
dorsal bands edged with light-colored tubercles	partly	partly	no	partly	yes	yes	no	no	variable	no
shape of dorsal bands	zig-zag	zig-zag	jagged	highly variable	highly variable	jagged	jagged	jagged	jagged	jagged
dark markings in dorsal interspaces in adults	yes	yes	yes	yes	yes	yes	yes	yes	yes	yes
ventrolateral body fold whitish	no	no	faintly	no	no	no	yes	no	no	no
light caudal bands bearing dark markings in adults	yes	yes	no	no	no	yes	yes	no	yes	yes
light caudal bands encircle tail	no	no	no	yes	no	no	no	no	no	no
mature regenerated tail spotted	no	no	/	no	/	no	no	yes	no	no
maximum SVL (mm)	83.0	82.0	69.3	87.0	74.0	91.6	70.6	84.1	76.3	66.9

Description of holotype. Adult male SVL 75.0 mm; head moderate in length (HL/SVL 0.29), wide (HW/HL 0.62), flat (HD/HL 0.37), distinct from neck, triangular in dorsal profile; lores inflated, prefrontal region concave, canthus rostralis rounded; snout elongate (ES/HL 0.38), rounded in dorsal profile, broad in lateral profile; eye large (ED/HL 0.25); ear opening oval (EL/HL 0.12); eye to ear distance greater than diameter of eye; rostral rectangular, partially divided dorsally, bordered posteriorly by supranasals that contact on midline, laterally by first supralabials; external nares bordered anteriorly by rostral, dorsally by supranasals, posteriorly by two relatively large postnasals, and ventrally by first supralabials; 9(R,L) rectangular supralabials extending to below midpoint of eye; 7(R,L) infralabials tapering posteriorly to commissure of jaw; scales of rostrum and lores slightly raised, larger than granular scales on top of head and occiput; scales on top of head and occiput intermixed with tubercles; dorsal superciliaries weakly pointed and directed posteriorly; mental triangular, bordered laterally by first infralabials and posteriorly by large left and right trapezoidal postmentals which contact medially for 60% of their length posterior to mental; two rows of enlarged chinshields, outermost row bordering first five infralabials; gular and throat scales granular, grading posteriorly into larger, subimbricate pectoral and ventral scales.

Body relatively short (AG/SVL 0.39) with well-defined ventrolateral folds; dorsal scales small, raised and interspersed with large, raised, semi-regularly arranged, strongly keeled tubercles; tubercles extend from top of head onto base of tail just beyond the postcloacal swelling; tubercles on nape smaller than those on body; 35 paravertebral tubercles; approximately 20 longitudinal rows of dorsal tubercles; 26 flat, subimbricate, ventral scales larger than dorsal scales; nine enlarged precloacal scales; three rows of large, post-precloacal scales; and no deep precloacal groove or depression.

Forelimbs moderate in stature, relatively short (FL/SVL 0.17); slightly raised, juxtaposed scales of forearm larger than those on body, intermixed with large tubercles; palmar scales slightly raised; digits well-developed, relatively long, inflected at basal, interphalangeal joints; digits much more narrow distal to inflections; widened proximal subdigital lamellae do extend onto palm; slight webbing at base of digit; claws well-developed, sheathed by a dorsal and ventral scale at base; hind limbs more robust than forelimbs, moderate in length (TBL/SVL 0.19), covered dorsally by small, raised, juxtaposed scales intermixed with large pointed tubercles and bearing flat, slightly larger imbricate scales anteriorly; ventral femoral scales flat, imbricate, much larger than dorsals; one row of

12(R)13(L) enlarged femoral scales and enlarged precloacal scales continuous; enlarged femoral scales nearly equal in size; small, postfemoral scales form an abrupt union with larger, flat ventral scales on posteroventral margin of thigh; eight(R) and seven(L) femoral pores; subtibial scales flat, imbricate; plantar scales raised; digits relatively long, well-developed, inflected at basal, interphalangeal joints; 10 (R,L) transversely expanded subdigital lamellae on fourth toe proximal to joint inflection that do not extend onto sole, 13 (R,L) unmodified subdigital lamellae distal to inflection; and claws well-developed, base of claw sheathed by a dorsal and ventral scale.

Tail complete, original, gracile in proportions, 96.0 mm in length, 7.4 mm in width at base, tapering to a point, TL/SVL (1.28); dorsal scales of tail flat, not forming distinct whorls; median row of transversely expanded subcaudal scales three times as wide as long, extending onto lateral subcaudal region; three enlarged postcloacal tubercles at base of tail on hemipenal swellings; and postcloacal scales flat.

Coloration in life during dark phase (Fig. 8). Dorsal ground color of body, limbs, and tail light-brown; ground color of top of head and rostrum light-yellow; top of head and rostrum bearing dark-colored, diffuse speckling; nuchal loop protracted posteriorly, divided medially, and bearing dark-colored, triangular occipital marking; no dark-colored band on nape; six irregularly shaped (zig-zag) body bands (some having paravertebral elements) bearing lightened centers and partly edged with whitish tubercles extending from the shoulder to the presacral region; lighter colored interspaces between bands bear darker markings; whitish tubercles scattered on flanks; sacral and postsacral band continue onto the tail to form nine black caudal bands that are wider than nine white caudal bands; white caudal bands bear dark markings and do not encircle tail; limbs bear faint, dark-colored bands and semi-transversely arranged yellowish spots; gular scales bearing only two or three black stipples; black stippling in throat, pectoral region, and anterior portion of belly much more dense; subcaudal region dark-colored with small amounts of whitish mottling.

Variation (Fig. 6, 8). The paratypes closely resemble the holotype in all aspects of coloration and pattern. Female paratype LSUHC 14203 is slightly darker overall and has dark coloration on the top of the head. Male paratype 14202 is lighter overall and has a more irregular banding pattern. Additional variation in meristic and mensural characters are presented in Table 7.

Distribution. Cyrtodactylus dattkyaikensis **sp. nov.** is known only from the type locality Datt Kyaik Hill, Kayin State, Myanmar (Fig. 2).

Etymology. The specific epithet, *dattkyaikensis* is a noun in apposition in reference to the type locality of Datt Kyaik Hill.



FIGURE 9. Microhabitat of *Cyrtodactylus dattkyaikensis* **sp. nov.** at Datt Kyaik Hill, Kayin State, Myanmar. Photograph by E. S. H. Quah.

TABLE 7. Meristic, mensural, and color pattern data from the type series of *Cyrtodactylus dattkyaikensis* **sp. nov.** R = right, L = left, / = data unobtainable or not applicable, r = regenerated.

	LSUHC	LSUHC	LSUHC
	14201	14202	14203
	Datt Kyaik	Datt Kyaik	Datt Kyaik
Sex	m	m	f
Supralabials	9	8	8
Infralabials	7	6	6
Body tubercles low, weakly keeled	no	no	no
Body tubercles raised, moderately to strongly keeled	yes	yes	yes
Paravertebral tubercles	35	33	34
Longitudinal rows of body tubercles	20	18	19
Tubercles extend beyond base of tail	yes	yes	yes
Ventral scales	26	25	25
Expanded subdigital lamellae on 4th toe	10	9	9
Unmodified subdigital lamellae on 4th toe	13	13	13
Total subdigital lamellae on 4th toe	23	22	22
Enlarged femoral scales (R/L)	R12L13	R13L12	R14L14
Total femoral scales	25	25	28
Femoral pores (R/L)	R8L7	R8L7	/
Total femoral pores in males	15	15	/
Enlarged precolacal scales	9	9	8
Precloacal pores	8	6	/
Post-precloacal scale rows	3	3	3
Enlarged femoral and precloacal scales continuous	yes	yes	yes
Pore-bearing femoral and precloacal scales continuous	no	no	/
Enlarged proximal femoral scales ~1/2 size of distal femorals	no	no	no
Medial subcaudals 2 or 3 times wider than long	yes	yes	yes
Medial subcaudals extend onto lateral surface of tail	yes	yes	yes
Nuchal loop divided medially	yes	yes	yes
2 posterior projections from nuchal loop	no	no	no
Nuchal loop with anterior azygous notch	no	no	no
Triangular marking anterior to nuchal loop	yes	yes	yes
Posterior border of nuchal loop	protracted	protracted	protracted
Band on nape	no	no	no
Dorsal banding with paravertebral elements	some	no	no
Number of body bands	~6	~6	~6
Dorsal body bands wider than interspaces	yes	yes	yes
Dorsal body bands with lightened centers	yes	yes	yes
Dorsal bands edged with white tubercles	partly	partly	partly
Shape of dorsal bands	zig-zag	zig-zag	zig-zag
Dark markings in dorsal interspaces	yes	yes	yes
Ventrolateral fold whitish	no	no	no
Top of head diffusely mottled, blotched, or patternless	mottled	mottled	blotched
Light-colored reticulum on top of head	no	no	no
Anterodorsal margin of thighs darkly pigmented	no	no	no

TABLE 7. (Continued)

	LSUHC	LSUHC	LSUHC
	14201	14202	14203
	Datt Kyaik	Datt Kyaik	Datt Kyaik
Anterodorsal margin of brachia darkly pigmented	no	no	no
White caudal bands with dark markings	yes	yes	/
White caudal bands encircle tail	no	no	/
Number of light-colored caudal bands	9	7	/
Number of dark-colored caudal bands	9	8	/
Dark-colored caudal bands wider than light-colored caudal bands	yes	/	/
Mature regenerated tail spotted	/		no
SVL	75.0	65.0	83.0
ΓL	96.0	84.0	68.0r
ΓW	7.4	5.9	7.3
FL	12.4	10.4	12.1
ГВГ	14.2	13.4	14.8
AG	29.3	23.6	33.3
HL	22.0	19.9	25.1
HW	13.6	12.6	15.5
HD	8.1	6.9	8.8
ED	5.6	5.1	5.5
EE	5.7	5.3	6.6
ES	8.3	7.8	89.0
EN	6.7	6.1	7.8
0	5.2	5.3	6.6
EL	2.6	2.5	2.6
IN	2.4	2.4	2.4

Natural history. Datt Kyaik Hill is small, karstic terrane situated on the south bank of the Donthami River approximately 1.2 km long, 725 m wide and reaching 123 m in elevation. Most of hill is covered with natural vegetation but the lower slopes support agricultural endeavors. There is a small cave at the northern end of the hill that lacks the appropriate fissures and cracks necessary to support *Cyrtodactylus*. The hillsides, however, are jagged and have deeply incised walls and alcoves bearing cracks, holes, and fissures creating suitable microhabitat (Fig. 9). Several specimens were seen at night on the walls and rocks near cracks and holes but only three were collected. The geckos were extremely wary and would rapidly and irretrievably take refuge as soon as they were hit with light. *Gekko gecko* (Linnaeus) and *Trimeresurus albolabris* Gray, both likely predators, were abundant which may explain why the *Cyrtodactylus* were so wary.

Comparisons (Tables 4, 6). Cyrtodactylus dattkyaikensis sp. nov. (n=3) differs from various combinations of all other species in the *C. sinyineensis* group (n=3–24) in having statistically different mean values across a broad number of scale characteristics (Table 4). It differs further from *C. chaunghanakwaensis* in having raised and more strongly keeled dorsal tubercles, discontinuous pore-bearing femoral and precloacal scales, no band on the nape, and the dorsal bands lacking paravertebral elements. It differs further from *C. dammathetensis* in having discontinuous pore-bearing femoral and precloacal scales, all femoral scales similarly sized, no band on the nape, and the dorsal bands lacking paravertebral elements, dorsal bands bearing lightened centers and being partly edged with light-colored tubercles, light-colored caudal bands bearing dark-colored markings, and a maximum SVL of 83.0 mm vs 69.3 mm (n=3). From *C. aequalis* it differs in that the median subcaudal scales extend onto the lateral side of the tail, lacking a band on the nape, body bands lacking paravertebral elements but bearing lightened centers, and no dark-colored markings in the light-colored caudal bands. From *C. cf. aequalis* it differs in that the median subcaudal scales do not extend onto the lateral side of the tail and the light-colored caudal bands do not encircle

the tail. From *C. sinyineensis* it differs in that the median subcaudal scales do not extend onto the lateral side of the tail and by lacking a band on the nape. It differs from *C. welpyanensis* in that the median subcaudal scales extend onto the lateral side of the tail and by lacking a band on the nape, having dorsal bands with lightened centers and being partly edged with light-colored tubercles, and not having a whitish ventrolateral fold. It differs from *C. bayinnyiensis* by lacking a band on the nape, having dorsal body bands partly edged with light-colored tubercles, the light-colored caudal bands bearing dark-colored markings, and the mature regenerated tail not spotted. From *C. naungnkayaingensis* it differs in that the dorsal bands lack paravertebral elements, are partly edged with light-colored tubercles, wider than the interspaces, and the maximum SVL length being 83.0 mm vs 66.9 mm (n=24). From *C. taungwineensis*, it differs in that the nuchal loop is divided.

Cyrotodactylus taungwineensis sp. nov. Taung Wine Hill Bent-toed Gecko (Figs. 7, 10, 11)

Holotype. Adult male LSUHC 14105 was collected on 6 November 2018 at 2100 hrs by Evan S. H. Quah, Myint Kyaw Thura, Jamie R. Oaks, Perry L. Wood Jr., Lin, A., and L. Lee Grismer from Taung Wine Hill, Kayin State, 12.4 km east of Hpa-an, Kayin State, Myanmar (16.90932°N, 97.74842°E; 31 m in elevation).

Paratypes. Adult male paratypes LSUHC 14108, 14110, 14112–15 and adult female paratypes 14106–07, 14109, 14111, bear the same collection data as the holotype.

Additional specimens examined. Juveniles LSUHC 14116–18 bear the same collection data as the holotype.

Diagnosis. *Cyrtodactylus taungwineensis* **sp. nov.** differs from all species in the *C. sinyineensis* group by having the combination of 7–10 supralabials; 6–8 infralabials; 29–32 paravertebral tubercles; 18–20 longitudinal rows of dorsal tubercles; 30–36 ventral scales; seven or eight expanded subdigital lamellae on the fourth toe; 11–13 unexpanded subdigital lamellae on the fourth toe; 18–21 total subdigital lamellae on the fourth toe; 19–30 enlarged femoral scales; a total of 13–22 pore-bearing femoral scales in males; 7–10 enlarged precloacal scales; 6–8 pore-bearing precloacal scales in males; three rows of enlarged post-precloacal scales; four or five dorsal body bands; 11–13 light-colored caudal bands; 11–13 dark-colored caudal bands; raised and strongly keeled dorsal tubercles that extend beyond the postcloacal swelling; enlarged femoral and precloacal scales nearly the same size and variably continuous; pore-bearing femoral and precloacal scales generally not continuous; medial subcaudals two to three times wider than long and not extending onto lateral side of tail; nuchal loop not divided medially, lacking an anterior azygous notch, and bearing a straight posterior border; no band on nape; dorsal bands lacking paravertebral elements, wider than interspaces, bearing lightened centers, partly edged with white tubercles, and generally zig-zag in shape; dark markings in dorsal interspaces; light-colored caudal bands in adults bearing dark-colored markings; light-colored caudal bands not encircling tail; and mature regenerated tail not spotted (Table 6).

Description of holotype. Adult male SVL 80.0 mm; head moderate in length (HL/SVL 0.28), wide (HW/HL 0.66), flat (HD/HL 0.38), distinct from neck, triangular in dorsal profile; lores inflated, prefrontal region concave, canthus rostralis rounded; snout elongate (ES/HL 0.40), rounded in dorsal profile, broad in lateral profile; eye large (ED/HL 0.24); ear opening oval (EL/HL 0.14); eye to ear distance greater than diameter of eye; rostral rectangular, partially divided and concave dorsally, bordered posteriorly by supranasals that do not contact on midline and one small azygous scale, laterally by first supralabials; external nares bordered anteriorly by rostral, dorsally by supranasals, posteriorly by two relatively large postnasals, and ventrally by first supralabials; 9(R,L) rectangular supralabials extending to below midpoint of eye; 7(R,L) infralabials tapering posteriorly to commissure of jaw; scales of rostrum and lores slightly raised, larger than granular scales on top of head and occiput; scales on top of head and occiput intermixed with tubercles; dorsal superciliaries weakly pointed and directed posteriorly; mental triangular, bordered laterally by first infralabials and posteriorly by large left and right trapezoidal postmentals which contact medially for 70% of their length posterior to mental; one row of enlarged chinshields bordering first six infralabials; gular and throat scales granular, grading posteriorly into larger, subimbricate pectoral and ventral scales.

Body relatively short (AG/SVL 0.38) with well-defined ventrolateral folds; dorsal scales small, raised and interspersed with large, raised, semi-regularly arranged, strongly keeled tubercles; tubercles extend from top of head onto base of tail slightly beyond the postcloacal swelling; tubercles on nape smaller than those on body; 30 paravertebral tubercles; approximately 19 longitudinal rows of dorsal tubercles; 36 flat, subimbricate, ventral scales larger

than dorsal scales; seven enlarged precloacal scales all bearing pores; three rows of large, post-precloacal scales; and no deep precloacal groove or depression.

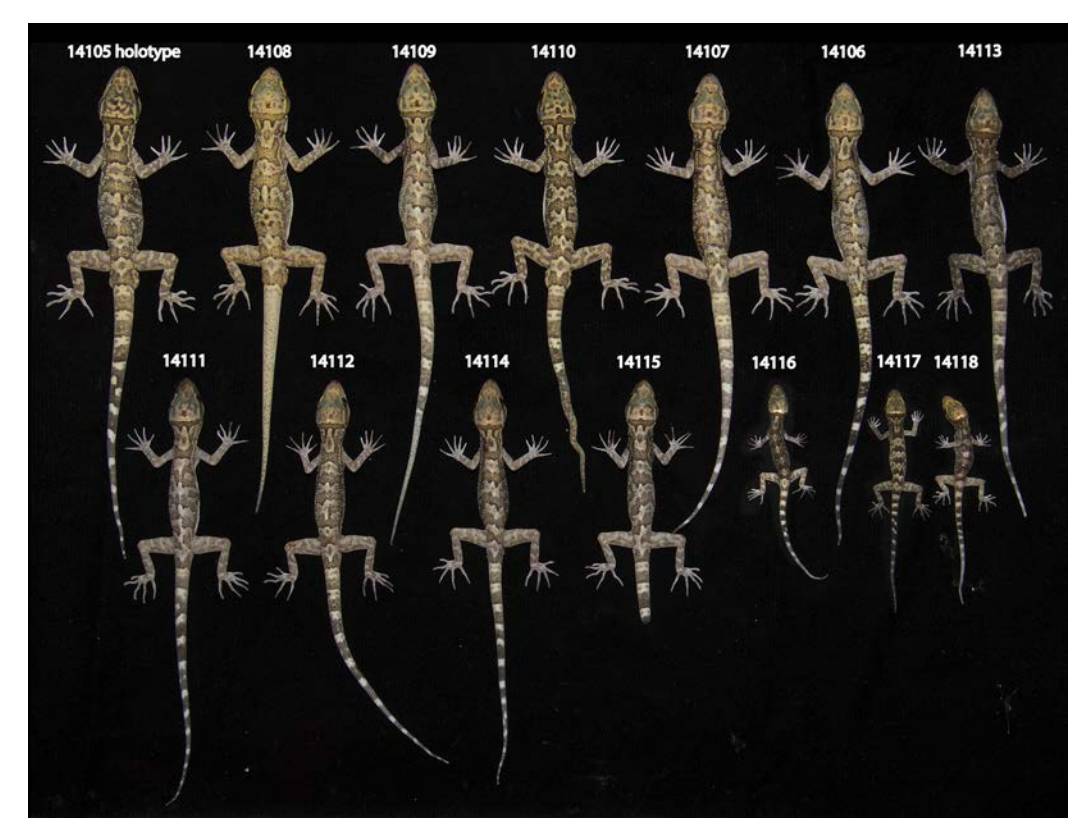


FIGURE 10. Dorsal coloration and pattern variation of the specimens of the type series of *Cyrtodactylus taungwineensis* **sp. nov.** just after euthenization and prior to preservation. Photograph by L. L. Grismer.

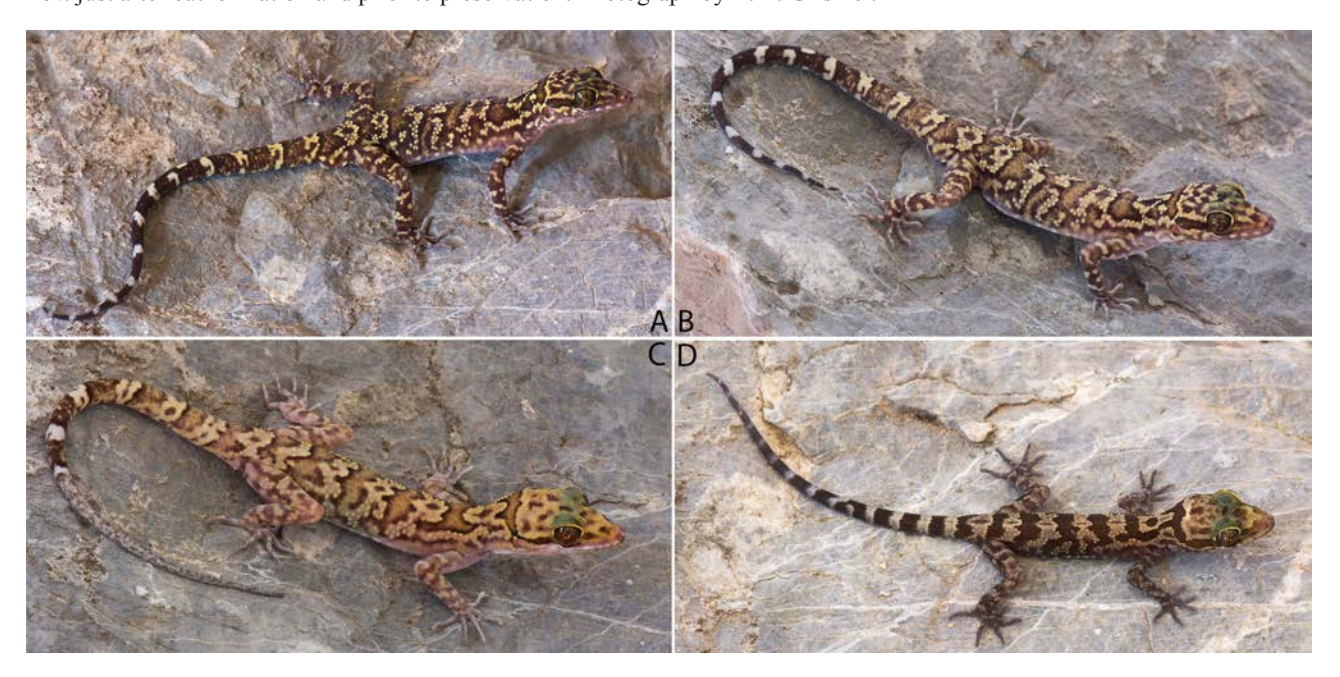


FIGURE 11. *Cyrtodactylus taungwineensis* **sp. nov.** from Taung Wine Hill, Kaying State, Myanmar. A and B. Adult male holotype LSUHC 14105 in dark and light phase, respectively. C. Adult female paratype LSUHC 14109 in light phase. D. Juvenile LSUHC 14117. Photographs by L. L. Grismer.

Forelimbs moderate in stature, relatively short (FL/SVL 0.15); slightly raised, juxtaposed scales of forearm larger than those on body, not intermixed with large tubercles; palmar scales slightly raised; digits well-developed, relatively long, inflected at basal, interphalangeal joints; digits much more narrow distal to inflections; widened

proximal subdigital lamellae extend onto palm; slight webbing at base of digits; claws well-developed, sheathed by a dorsal and ventral scale at base; hind limbs more robust than forelimbs, moderate in length (TBL/SVL 0.20), covered dorsally by small, raised, juxtaposed scales intermixed with large pointed tubercles and bearing flat, slightly larger imbricate scales anteriorly; ventral femoral scales flat, imbricate, much larger than dorsals; one row of 7(R)15(L) enlarged femoral scales and enlarged precloacal scales continuous on left side only; enlarged femoral scales nearly equal in size on right side, anomalously small on left side; small, postfemoral scales form an abrupt union with larger, flat ventral scales on posteroventral margin of thigh; seven(R) and eight(L) femoral pores; subtibial scales flat, imbricate; plantar scales raised; digits relatively long, well-developed, inflected at basal, interphalangeal joints; 8(R,L) transversely expanded subdigital lamellae on fourth toe proximal to joint inflection that do not extend onto sole, 12(R,L) unmodified subdigital lamellae distal to inflection; and claws well-developed, base of claw sheathed by a dorsal and ventral scale.

Tail complete, original, gracile in proportions, 110.0 mm in length, 10.0 mm in width at base, tapering to a point, TL/SVL (1.88); dorsal scales of tail flat, not forming distinct whorls; median row of transversely expanded subcaudal scales three times as wide as long, not extending onto lateral subcaudal region anteriorly, twice as wide as long posteriorly and not extending onto lateral surface of tail; three enlarged postcloacal tubercles at base of tail on hemipenal swellings; and postcloacal scales flat.

Coloration in life during dark phase (Fig. 11). Dorsal ground color of head, body, limbs, and anterior portion of tail dull-yellow; top of head and rostrum bearing dark-colored irregularly shaped blotches; dark-colored nuchal loop not divided medially or bearing an anterior notch or dark-colored triangular blotch; no band on nape; five zigzag shaped body bands bearing lightened centers, and partly edged with white tubercles; sacral, and postsacral bands irregularly shaped, bearing lightened centers, and edged with white tubercles, extending onto tail to form three brown bands anteriorly and 10 black bands posteriorly all wider than the light-colored caudal bands; 13 light-colored caudal bands bearing dark markings and not encircling tail; limbs bearing wide dark-colored bands separated by narrow, irregularly shaped, yellowish bands; gular scales bearing only two or three black stipples; black stippling on throat, pectoral region, and anterior portion of belly much more dense; subcaudal region dark-colored with small amounts of whitish mottling. Figure 11B is the holotype in its light phase.

Variation (Fig. 10). The paratypes generally resemble the holotype in all aspects of dorsal coloration and pattern. LSUHC 14110 has a bolder, more contrasting color pattern and the banding pattern in paratypes 14107 and 14111 is more irregular. Juveniles LSUHC 14116–18 are generally more boldly banded than adults. LSUHC 14108 has a regenerated tail as are the posterior one-thirds of the tails of LSUHC 14109–10. That of LSUHC 14115 is broken. Additional variation in meristic and mensural characters are presented in Table 8.

Distribution. *Cyrtodactylus taungwineensis* **sp. nov.** is known only from the type locality Taung Wine Hill, Kayin State, Myanmar (Fig. 2).

Etymology. The specific epithet, *taungwineensis* is a noun in apposition in reference to the type locality of Taung Wine Hill.

Natural history. Taung Wine Hill is a small, irregularly shaped karstic terrane 1.3 km by 993 m that reaches 260 m in elevation. At the northern end of the hill is a large bowl-shaped alcove in which there is a small monastery. The sides of the hill are covered by a dense karst forest and the limestone is rugged, deeply eroded, and bearing many cracks, fissures, holes, and scattered boulders (Fig. 12). *Cyrtodactylus taungwineensis* **sp. nov.** were common at night and adults were as prevalent on the vegetation from 0.03–2m above the ground as on karst. Small juveniles were found only on the ground. No hatchlings or gravid females were observed, suggesting that November is past the reproductive season.

Comparisons (Tables 4, 6). Cyrtodactylus taungwineensis sp. nov. (n=14) differs from various combinations of all other species in the *C. sinyineensis* group (n=3–24) in having statistically different mean values across a broad number of scale characteristics (Table 4). It differs from *C. dammathetensis* in having similarly sized enlarged femoral scales, medial subcaudal scales not extending onto the lateral side of the tail, lacking a band on the nape, dorsal bands lacking paravertebral elements but with lightened centers and partly edged with light-colored tubercles, light-colored caudal bands bearing dark-colored markings in adults, and a maximum SVL of 82.0 mm vs 69.3 mm (n=3). From *C. aequalis* it differs in not having a medially divided nuchal loop, lacking a band on the nape, dorsal bands lacking paravertebral elements but with lightened centers, having light-colored caudal bands that do not encircle the tail that bear-colored dark markings in adults. It differs from *C. cf. aequalis* in that the light-colored caudal bands in adults have dark-colored markings. From *C. sinyineensis* it differs in lacking a band on the nape. It differs from *C. welpyanensis*

by lacking a band on the nape, having dorsal bands with lightened centers that are partly edged with light-colored tubercles, and by not having a whitish ventrolateral body fold. It can be separated from *C. bayinnyiensis* in that the median subcaudal scales do not extend onto the lateral side of the tail, it lacks a band on the nape, the dorsal bands are partly edged with light-colored tubercles, there are dark-colored markings in the light-colored caudal bands, and the mature regenerated tail is not spotted. It is differentiated from *C. chaunghanakwaensis* in that the dorsal tubercles are larger and more strongly keeled, the pore-bearing femoral and precloacal scales are discontinuous, the median subcaudal scales do not extend onto the side of the tail, there is no band on the nape, and there are no paravertebral elements in the dorsal bands. From *C. naungkayaingensis* it is separated by the median subcaudal scales not extending onto the side of the tail, no paravertebral elements in the dorsal bands, the dorsal bands being wider than the interspaces and partly edged with light-colored tubercles, and having a maximum SVL of 82.0 mm vs 66.9 mm (n=3).



FIGURE 12. Forest habitat and karstic microhabitat of *Cyrtodactylus taungwineenensis* **sp. nov.** at Taung Wine Hill, Kayin State, Myanmar. Photograph by L. L. Grismer.

Remarks on the taxonomy of Cyrtodactylus aequalis

Cyrtodactylus aequalis was described on the basis of single specimen from the Kyaiktiyo Wildlife Sanctuary, Mon State at 382 m in elevation (Bauer 2003). Grismer et al. (2018a) reported on a second specimen from a granite outcrop at 1073 m in elevation near the Golden Rock Pagoda and indicated it was a member of the C. sinyineensis group and most closely related to C. dammathetensis. With the discovery of C. chaunghanakwaensis, C. naungkayaingensis, C. bayinnyiensis (Grismer et al. 2018b) and C. dattkyaikensis sp. nov. herein, the phylogenetic analyses based on 13 additional samples of C. aequalis from >1000 m in elevation indicate it is most closely related to the sister species C. bayinnyiensis and C. dattkyaikensis sp. nov. We also discovered a lowland granite-associated population of Cyrtodactylus from Kay Lar Tha—a small granitic hill approximately 25 km south of the type locality of C. aequalis (Fig. 2)—composed of individuals that superficially resemble C. aequalis (Fig. 13). Three specimens were found on granite rocks and another on the trunk of a tree near granite rocks. Despite this population being most closely related to C. aequalis (Fig. 3) and separated by only a 1.1% uncorrected pairwise sequence divergence (Table 5), it differs significantly by having fewer expanded to lamellae on the fourth toe (seven or eight, x=7.5, n=4 vs 7-10, x=8.8, n=16), fewer paravertebral tubercles (29, x=29.0, n=4 vs 31-36, x=33.3, n=16), and a smaller maximum SVL with a gravid female (LSUHC 14243) reaching 74.0 mm (n=4) vs 90.0 mm (Bauer 2003). Given that these two populations are reciprocally monophyletic and are morphologically diagnosable, one could forward an argument for their separate specific recognition. However, their low sequence divergence and the possibility of gene flow through low, hilly areas to the east, lead us to recognize the Kay Lar Tha population as C. cf. aequalis. An expedition to the low hills to the east is planned.

TABLE 8. Meristic, mensural, and color pattern data from the type series of Cyrtodactylus taungwineensis sp. nov. R = right, L = left, / = data unobtainable or not ap-

	LSUHC	LSUHC	LSUHC											
	14105	14106	14107	14108	14109	14110	141111	14112	14113	14114	14115	14116	14117	14118
	Taung Wine	Taung Wine	Taung Wine											
Sex	ш	f	f	ш	f	ш	t.	ш	E	Е	ш			
Supralabials	6	6	10	7	6	10	6	10	∞	6	6	6	6	10
Infralabials	7	7	∞	9	7	7	7	7	7	7	7	7	7	7
Body tubercles low, weakly keeled	ou	ou	ou	ou	no	ou	ou	ou	ou	ou	no	no	no	ou
Body tubercles raised, moderately to strongly keeled	yes	yes	yes											
Paravertebral tubercles	30	32	30	30	30	31	32	30	30	29	30	31	30	30
Longitudinal rows of body tubercles	19	18	19	18	19	19	19	18	19	18	19	20	19	18
Tubercles extend beyond base of tail	yes	yes	yes											
Ventral scales	36	36	31	31	31	30	33	32	34	34	30	31	31	32
Expanded subdigital lamellae on 4th toe	∞	7	7	∞	∞	7	∞	7	7	7	~	7	7	7
Unmodified subdigital lamellae on 4th toe	12	12	12	12	11	12	13	Π	12	12	13	12	12	13
Total subdigital lamellae on 4th toe	20	19	19	20	19	19	21	18	19	19	21	19	19	20
Enlarged femoral scales (R/L)	R7L15	R15L13	R14L12	R11L11	R15L15	R14L14	R11L11	R11L12	R8L12	R12L14	R12L12	R10L9	R9LDAM	R14L15
Total femoral scales	22	28	26	22	30	28	22	23	20	26	24	19	18	19
Femoral pores (R/L)	R7L8	\	_	R11L11	_	R10L9	_	R5L8	R6L8	R7L8	R8L8	. . .	R4L/	J
Total femoral pores in males	15	\	\	22	\	19	\	13	14	15	16	\	_	\
Enlarged Precolacal scales	7	6	6	∞	~	6	∞	6	~	∞	10	6	6	10
Precloacal pores	7	\	\	9	\	9	\	9	7	9	~	. –	3	
Post-precloacal scales rows	3	3	3	3	3	3	3	3	3	3	3	3	3	3
Enlarged femoral and precloacal scales continuous	no*	yes	yes	ou	yes	ou	ou	no	no	ou	yes	yes	ou	ou
Pore-bearing femoral and precloacal scales continuous	no	_	_	no	_	no	_	no	no	no	no	no	no	yes
Enlarged proximal femoral scales ~1/2 size of distal														
femorals	ou	no	ou											
Medial subcaudals 2 or 3 times wider than long	yes	yes	yes	\	yes	yes	yes							
Medial subcaudals extend onto lateral surface of tail	ou	ou	ou	\	no	ou	ou	ou	ou	ou	no	no	no	ou
Nuchal loop divided medially	ou	no	no	no	no	no	ou	no	no	no	no	no	no	no
2 posterior projections from nuchal loop	yes	yes	yes											

.... Continued on next page

IABLE 8. (Continued)														
	LSUHC	LSUHC	LSUHC	LSUHC	LSUHC	LSUHC	LSUHC							
	14105	14106	14107	14108	14109	14110	14111	14112	14113	14114	14115	14116	14117	14118
	Taung	Taung	Taung	Taung	Taung	Taung	Taung							
	Wine	Wine	Wine	Wine	Wine	Wine	Wine							
Nuchal loop with anterior azygous notch	ou	no	ou	no	no	no	ou	no	ou	ou	no	no	no	no
Triangular marking anterior to nuchal loop	ou	ou	ou	no	ou	no	no	no	ou	ou	no	no	no	no
Posterior border of nuchal loop	straight	straight	straight	straight	straight	straight	straight							
Band on nape	no	no	no	no	ou	no	no	no	no	no	no	no	no	no
Dorsal banding with paravertebral elements	no	no	no	no	ou	no	no	no	no	no	no	no	no	no
Number of body bands	5	4	4	4	4	4	4	4	4	4	4	4	4	4
Dorsal body bands wider than interspaces	yes	yes	yes	yes	yes	equal	equal							
Dorsal body bands with lightened centers	yes	yes	yes	yes	yes	no	ou							
Dorsal bands edged with white tubercles	partly	partly	partly	partly	partly	partly	partly							
Shape of dorsal bands	zig-zag	zig-zag	zig-zag	zig-zag	zig-zag	zig-zag	zig-zag							
Dark markings in dorsal interspaces	yes	yes	yes	yes	yes	yes	yes							
Ventrolateral fold whitish	ou	ou	ou	ou	ou	no	no							
Top of head diffusely mottled, blotched, or	14 6	4	140	770	17	17	17	1 6 1 7 7 7 7 7 7 7 7 7 7 7 7 7 7 7 7 7	140	177	140	177	1	-
patterniess	mottled	mottled	mottled	mottled	mottled	unicolor	unicolor							
Light-colored reticulum on top of head	ou	no	ou	no	ou	no	no	no	ou	no	no	ou	ou	no
Anterodorsal margin of thighs darkly pigmented	no	ou	no	ou	ou	no	no	ou	ou	no	ou	ou	no	no
Anterodorsal margin of brachia darkly pigmented	ou	ou	ou	ou	no	ou	no							
White caudal bands with dark markings	yes	yes	yes	\	yes	yes	yes	yes	yes	yes	yes	yes	ou	ou
White caudal bands encircle tail	ou	ou	ou	_	ou	no	no	no	ou	ou	no	no	no	no
Number of light caudal bands	13	12	11	\	\	\	12	12	12	12	_	\	12	13
Number of dark caudal bands	13	12	11	\	\	\	12	12	11	12	\	_	12	13
Dark caudal bands wider than light caudal bands	yes	yes	yes	\	yes	yes	yes	yes	yes	yes	yes	yes	yes	yes
Mature regenerated tail spotted	\	\	_	no	ou	no	\	\	_	_	\	\	_	
TAS	80.0	78.0	82.0	80.0	80.0	0.67	0.79	0.79	72.0	65.0	0.99	39.0	40.0	38.0
TL	110	102	102	93	107	86r	96	96	93	06	30b	45	48	46
TW	9.95	7.18	7.01	8.37	99.7	9.44	5.91	5.32	6.25	6.38	90.9	2.64	2.68	2.7
FL	11.98	12.72	13.03	12.68	12.85	12.58	10.19	62.6	11.3	96.6	88.6	5.47	5.27	5.14
													;	

14118 6.34 14117 Taung 14.14 12.3 3.43 6.7 4.81 LSUHC 14116 86.9 4.28 4.67 14.5 3.05 3.87 3.23 6.87 4.02 LSUHC 7.81 LSUHC 14.04 LSUHC Taung 13.9 19.31 96.9 8.01 8.26 96.6 LSUHC 16.58 14.41 4.91 LSUHC 14.57 4.91 6.91 Faung Wine 16.29 30.55 14.76 8.58 6.01 8.94 TABLE 8. (Continued) HМ HD ED ES EN 0

....Continued on next page

180 · *Zootaxa* 4718 (2) © 2020 Magnolia Press

Discussion

The work herein builds on that of Grismer *et al.* (2018a,b) and continues to underscore the archipelago-like nature of the karstic landscape of the Salween Basin not only in terms of geomorphology but in terms of island biogeography where some islands have been colonized multiple times by unrealted species from different clades, some adjacent islands are inhabited by the same species, and yet other islands harbor only a single endemic species. The mode and timing of the colonization of these landscapes is under review be it vicariance or dispersal. Grismer *et. al.* (2018c)—based on a mitochondrial data set—proposed that the Salween Basin was invaded 23.3 mya and subsequently gave rise to the six other species groups of eastern Myanmar and Indochina over approximately the next 12 million years. The biogeography and speciation within these groups will be addressed with a forthcoming genomic data set.

Given the number of new karst-associated species of *Cyrtodactylus* (26) and *Hemiphyllodactylus* Bleeker, 1860 (five species) that have been described in Myanmar since 2017 (Grismer *et al.* 2017, 2018a,b,c,d,e,f,g, 2019a,b; Connete *et al.* 2018), reports such as these have become an expectation rather than a surprise. The over-arching benefit of these discoveries, however, is that systematic herpetologists are now regarding karstic microhabitats throughout Southeast Asia as "hot-beds" of speciation as well as sources of refuge and endemism and not just "Arks of Biodiversity" harboring relic plants and invertebrates (see discussions in Grismer 2017a,b, 2018a,b; Grismer *et al.* 2014, 2016, 2018b). As such, arguments for the conservation of these species have become more persuasive and in August of 2019, an IUCN committee met to assess the status of all karst-associated gekkonids in Myanmar.

Acknowledgments

We wish to thank Mr. Win Naing Thaw of the Ministry of Natural Resources and Environmental Conservation Forest Department for the collection and export permits. LLG thanks the College of Arts and Sciences of La Sierra University and Fauna & Flora International for partial funding. JRO was supported by funding from the National Science Foundation of the USA (DEB 1656004). This paper is contribution number 906 of the Auburn University Museum of Natural History.

References

- Agarwal, I., Bauer, A.M., Jackman, T.R. & Karanth, K.P. (2014) Insights into Himalayan biogeography from geckos: a molecular phylogeny of *Cyrtodactylus* (Squamata: Gekkonidae). *Molecular Phylogenetics and Evolution*, 80, 145–155. https://doi.org/10.1016/j.ympev.2014.07.018
- Barraclough, T.G., Birky, C.W. Jr. & Burt, A. (2003) Diversification in sexual and asexual organisms. *Evolution*, 57, 2166–2172. https://doi.org/10.1111/j.0014-3820.2003.tb00394.x
- Bauer, A.M. (2003) Descriptions of seven new *Cyrtodactylus* (Squamata: Gekkonidae) with a key to the species of Myanmar (Burma). *Proceedings of the California Academy of Sciences*, 54, 463–498.
- Connette, G.M., Oswald, P., Thura, M.K., Connette, K.J.L., Grindley, M.E., Songer, M., Zug, G.R., Mulchay, D.G. (2017) Rapid forest clearing in a Myanmar proposed national park threatens two newly discovered species of geckos (Gekkonidae: *Cyrtodactylus*). *PLoS One*, 12, e0174432.
 - https://doi.org/10.1371/journal.pone.0174432
- Coyne, J.A. & Orr, H.A. (1998) The evolutionary genetics of speciation. *Philosophical Transactions of the Royal Society of London B*, 353, 287–305.
 - https://doi.org/0.1098/rstb.1998.0210
- De Queiroz, K. (2007) Species concepts and species delimitation. *Systematic Biology*, 56, 879–886. https://doi.org/10.1080/10635150701701083
- Fontaneto, D., Herniou, E.A., Boschetti, C., Caprioli, M., Melone, G., Ricci, C. & Barrenclough, T.G. (2007) Independently evolving species in asexual bdelloid rotifers. *PLoS Biology*, 5, e87. https://doi.org/10.1371/journal.pbio.0050087
- Grismer, L.L. (2017a) *Herpetofaunal Survey of the Pyinyaung Limestone Mining Area*. Unpublished survey report for Fauna & Flora International, Yangon, 12 pp.
- Grismer, L.L. (2017b) *Herpetofaunal Survey of Limestone Habitats in the Salween Basin*. Unpublished survey report for Fauna & Flora International, Yangon, 17 pp.
- Grismer, L.L. (2018a) *Herpetofaunal Survey of Karstic Habitats in the Salween Basin*. Unpublished survey report for Fauna & Flora International, Yangon, 13 pp.

- Grismer, L.L. (2018b) *Gecko Surveys of the Panlaung-Pyadalin Cave Wildlife Sanctuary and Adjacent Areas in Shan State and Mandalay Division*. Unpublished survey report for Fauna & Flora International, Yangon, 12 pp.
- Grismer, L.L., Wood Jr., P.L., Anuar, S., Davis, H.R, Cobos, A.J. & Murdoch, M.L. (2016) A new species of karst forest Benttoed Gecko (genus *Cyrtodactylus* Gray) not yet threatened by foreign cement companies and a summary of Peninsular Malaysia's endemic karst forest herpetofauna and the need for its conservation. *Zootaxa*, 4061 (1), 1–17. https://doi.org/10.11646/zootaxa.4061.1.1
- Grismer, L.L., Wood Jr., P.L., Chan, K.O., Anuar & Muin, M.A. (2014) Cyrts in the city: A new Bent-toed Gecko (Genus *Cyrtodactylus*) is the only endemic species of vertebrate from Batu Caves, Selangor, Peninsular Malaysia. *Zootaxa*, 3774 (4), 381–394.
 - https://doi.org/10.11646/zootaxa.3774.4.6
- Grismer, L.L., Wood Jr., P.L., Thura, M.K., Win, N.M. & Quah, E.S.H. (2018g) Two more new species of the *Cyrtodactylus peguensis* group (Squamata: Gekkonidae) from the fringes of the Ayeyarwady Basin, Myanmar. *Zootaxa*, 4577 (2), 274–294. https://doi.org/10.11646/zootaxa.4577.2.3
- Grismer, L.L., Wood Jr., P.L., Thura, M.K., Quah, E.S.H., Grismer, M.S., Murdoch, M.L., Espinoza, R.E. & Lin, A. (2018c) A new *Cyrtodactylus* Gray (Squamata, Gekkonidae) from the Shan Hills and the biogeography of Bent-toed Geckos from eastern Myanmar. *Zootaxa*, 4446 (4), 477–500. https://doi.org/10.11646/zootaxa.4446.4.4
- Grismer, L.L., Wood. Jr., P.L., Thura, M.K., Zin, T., Quah, E.S.H., Murdoch, M.L., Grismer, M.S., Lin, A., Kyaw, H. & Ngwe, L. (2018a) Twelve new species of *Cyrtodactylus* Gray (Squamata: Gekkonidae) from isolated limestone habitats in east-central and southern Myanmar demonstrate high localized diversity and unprecedented microendemism. *Zoological Journal of the Linnean Society*, 182, 862–959. http://doi.org/10.1093/zoolinnean/zlx057
- Grismer, L.L., Wood Jr., P.L., Thura, M.K., Win, N.M., Grismer, M.S., Trueblood, L.A. & Quah, E.H.S. (2018c) A re-description of *Cyrtodactylus chrysopylos* Bauer (Squamata: Gekkonidae) with comments on the adaptive significance of orange coloration in hatchlings and descriptions of two new species from eastern Myanmar (Burma). *Zootaxa*, 4527 (2), 151–185. https://doi.org/10.11646/zootaxa.4527.2.1
- Grismer, L.L., Wood Jr., P.L., Thura, M.K., Zin, T., Quah, E.S.H., Murdoch, M.L., Grismer, M.S., Herr, M.W., Lin, A. & Kyaw, H. (2018b) Three more new species of *Cyrtodactylus* (Squamata: Gekkonidae) from the Salween Basin of eastern Myanmar underscores the urgent need for the conservation of karst habitats. *Journal of Natural History*, 52, 1243–1294. http://doi.org/10.1080/00222933.2018.1449911
- Grismer, L.L., Wood Jr., P.L., Quah, E.S.H., Thura, M.K., Herr, M.X. & Lin, A.K. (2019b) A new species of forest-dwelling *Cyrtdactylus* (Squamata: Gekkonidae) from Indawgyi Wildlife Sanctuary, Kachin State, Myanmar. *Zootaxa*, 4623 (1), 1–25.
 - https://doi.org/10.11646/zootaxa.4623.1.1
- Grismer, L.L., Wood Jr., P.L., Quah, E.S.H., Thura, M.K., Murdoch, M.L., Grismer, M.S., Herr, M.W., Espinoza, R.E., Brown, R.M. & Lin, A. (2018e)Phylogenetic taxonomy of the *Cyrtodactylus peguensis* group (Reptilia: Squamata: Gekkonidae) with descriptions of two new species from Myanmar. *PeerJ*, 6, e5575. https://doi.org/10.7717/peerj.5575
- Grismer, L.L., Wood Jr., P.L., Thura, M.K., Zin, T., Quah, E.S.H., Murdoch, M.L., Grismer, M.S., Lin, A., Kyaw, H. & Ngwe, L. (2017) Phylogenetic taxonomy of *Hemiphyllodactylus* Bleeker, 1860 (Squamata: Gekkonidae) with descriptions of three new species from Myanmar. *Journal of Natural History*, 52, 881–195. https://doi.org/10.1080/00222933.2017.1367045
- Grismer, L.L., Wood Jr., P.L., Quah, E.S.H., Thura, M.K., Oaks, J.R. & Lin, A. (2019a) A new species of Bent-toed Gecko (Squamata, Gekkonidae, *Cyrtodactylus*) from the Shan Plateau in eastern Myanmar (Burma). *Zootaxa*, 4624 (3), 301–321. https://doi.org/10.11646/zootaxa.4624.3.1
- Grismer, L.L., Wood Jr., P.L., Zug, G.R., Thura, M.K., Grismer, M.S., Quah, E.S.H., Murdoch, M.L. & Lin, A. (2018d) Two more new species of *Hemiphyllodaxctylus* Bleeker (Squamata: Gekkonidae) from the Shan Hills of eastern Myanmar (Burma). *Zootaxa*, 4483 (2), 295–316. https://doi.org/10.11646/zootaxa.4483.2.4
- Hillis, D.M. (2019) Species delimitation in herpetology. *Journal of Herpetology*, 53, 3–12. https://doi.org/10.1670/18-123
- Hoang, D.T., Chernomor, O., von Haeseler, A., Minh, B.Q. & Vinh, L.S. (2018) UFBoot2: Improving the ultrafast bootstrap approximation. *Molecular Biology and Evolution*, 35, 518–522. https://doi.org/10.1093/molbev/msx281
- Huelsenbeck, J.P., Ronquist, F., Nielsen, R. & Bollback, J.P. (2001) Bayesian Inference of Phylogeny and Its Impact on Evolutionary Biology. *Science*, 294, 2310–2314. https://doi.org/10.1126/science.1065889
- Jombart, T., Devillard, S. & Balloux, F. (2010) Discriminant analysis of principal components: a new method for the analysis of genetically structured populations. *BMC Genetics*, 11, 94. https://doi.org/10.1186/1471-2156-11-94
- Kalyaanamoorthy, S., Minh, B.Q., Wong, T.K., von Haeseler, A. & Jermiin, L.S. (2017) ModelFinder: fast model selection for

- accurate phylogenetic estimates. Nature methods, 14, 587.
- https://doi.org/10.1038/nmeth.4285
- Katoh, M. & Kuma, M. (2002) MAFTT: a novel method for rapid sequence alignment based on fast Fourier transform. *Nucleic Acids Research*, 30, 3059–3066.
 - https://doi.org/10.1093/nar/gkf436
- Knowles, L.L. & Carstens, B.C. (2007) Delimiting species without monophyletic gene trees. *Systematic Biology*, 56, 887–895. https://doi.org/10.1080/10635150701701091
- Kumar, S., Stecher, G. & Tamura, K. (2016) MEGA7: Molecular evolutionary genetics analysis version 7.0 for bigger datasets. *Molecular Biology and Evolution*, 33, 1870–1874. https://doi.org/10.1093/molbev/msw054
- Leaché, A.D., Koo, M.S., Spencer, C.L., Papenfuss, T.J., Fisher, R.N. & McGuire, J.A. (2009) Quantifying ecological, morphological, and genetic variation to delimit species in the coast horned lizard species complex (*Phrynosoma*). *Proceedings of the National Academy of Sciences*, 106, 12418–12423. https://doi.org/10.1073/pnas.0906380106
- Macey, J.R., Larson, A., Ananjeva, N.B., Fang, Z. & Papenfuss, T.J. (1997) Two novel gene orders and the role of light-strand replication in rearrangement of the vertebrate mitochondrial genome. *Molecular Biology and Evolution*, 14 (1), 91–104. https://doi.org/10.1006/mpev.1997.0478
- Maddison, W.P. & Maddison, D.R. (2015) *Mesquite: a modular system for evolutionary analysis*. Version 3.04. Available from: http://mesquiteproject.org (accessed 01 August 2018)
- Miller, M.A., Pfeiffer, W. & Schwartz, T. (2010) Creating the CIPRES Science Gateway for inference of large phylogenetic trees. *Proceedings of the Gateway Computing Environments Workshop (GCE), New Orleans, Louisiana*, 14 November 2010, pp. 1–8. https://doi.org/10.1109/GCE.2010.5676129
- Minh, Q., Nguyen, M.A.T. & von Haeseler, A. (2013) Ultrafast approximation for phylogenetic bootstrap. *Molecular Biology and Evolution*, 30, 1188–1195. https://doi.org/10.1093/molbev/mst024
- Nguyen, L.-T., Schmidt, H.A., von Haeseler, A. & Minh, B.Q. (2015) IQ-TREE: A fast and effective stochastic algorithm for estimating maximum likelihood phylogenies. *Molecular Biology and Evolution*, 32, 268–274. https://doi.org/10.1093/molbev/msu300
- R Core Team (2018) R: A language and environment for statistical computing. R Foundation for Statistical Computing. Vienna. Available from: http://www.R-project.org (accessed 1 August 2018)
- Rambaut, A., Suchard, M.A., Xie, D. & Drummond, A.J. (2014) *Tracer: Version 1.6.* Available from: http://tree.bio.ed.ac.uk/software/tracer/ (accessec 13 November 2019)
- Ronquist, F., Teslenko, M., van der Mark, P., Ayres, D.L., Darling, A., Höhna, B., Larget, L., Liu, L., Suchard, M.A. & Huelsenbeck, J.P. (2012) Mr. Bayes 3.2: efficient Bayesian phylogenetic inference and model choice across a large model space. *Systematic Biology*, 61, 539–542. https://doi.org/10.1093/sysbio/sys029
- Sabaj, M.H. (2016) Standard symbolic codes for institutional resource collections in herpetology and ichthyology: an Online Reference. Version 6.5 (16 August 2016). American Society of Ichthyologists and Herpetologists, Washington, D.C. Available from: http://www.asih.org/ (accessed 01 October 2019)
- Trifinopoulos, J., Nguyen, L.-T., von Haeseler, A. & Minh, B.Q. (2016) W-IQ-TREE: a fast online phylogenetic tool for maximum likelihood analysis. *Nucleic Acids Research*, 44, W232–W235 https://doi.org/10.1093/nar/gkw256
- Wilcox, T.P., Zwickl, D.J., Heath, T.A. & Hillis, D.M. (2002) Phylogenetic relationships of the Dwarf Boas and a comparison of Bayesian and bootstrap measures of phylogenetic support. *Molecular Phylogenetics and Evolution*, 25, 361–371. http://doi.org/10.1016/S1055-7903(02)00244-0
- Wood Jr., P.L., Heinicke, M.P., Jackman, T.R. & Bauer, A.M. (2012) Phylogeny of bent-toed geckos (*Cyrtodactylus*) reveals a west to east pattern of diversification. *Molecular Phylogenetics and Evolution*, 65, 992–1003. https://doi.org/10.1016/j.ympev.2012.08.025